DYNAMICAL SYSTEMS ANALYSIS OF A TWO-LEVEL TROPHIC FOOD WEB IN THE SOUTHERN OCEANS

By

Scott Hadley, B.Sc. Hons (Tas)

Submitted in fulfilment of the requirements
for the Degree of Masters of Science.

School of Mathematics and Physics
University of Tasmania
July, 2009

I declare that this thesis contains no material which has been accepted for a degree or diploma by the University or any other institution, except by way of background information and duly acknowledged in this thesis., and that, to the best of my knowledge and belief, this thesis contains no material previously published or written by another person, except where acknowledged within the text of the thesis.

Signed: SQ Hadley

Date: 6/7/09

Signed: _____

Date: 6/7/09

ACKNOWLEDGEMENTS

I would like to sincerely express my thanks to Professor Larry Forbes, my supervisor for this publication. His patience, guidance and knowledge were the reason it has seen the light of day. I would also like to thank Karen Bradford for her help in organising my meetings and being both flexible and patient in this regard.

I would also like to thank the University of Tasmania in general for the opportunity to undertake this research. I am better for it.

ABSTRACT

A theoretical model developed by Stone describing a two level trophic system in the Ocean is analysed, for the case in which there is unlimited supply of nutrients. It is shown that spontaneous oscillations in population numbers are possible, but they do not arise from a Hopf bifurcation. Seasonal forcing of the model is also investigated, and it is shown that resonances can occur, in addition to highly nonlinear behaviour including high period oscillations, quasi-periodicity and chaos.

The model is then extended to include the case in which nutrient concentrations are allowed to vary. In this model seasonal forcing is not considered. Nevertheless a Hopf bifurcation is found for a critical value of the bifurcation parameter which is chosen as the non-dimensional reproductive rate of bacteria. The Hopf bifurcation gives rise to oscillatory solutions appearing as limit cycles. The stability of the limit cycles found is determined using Floquet theory, where it is observed that the periodic solutions arise from the Hopf bifurcation as stable orbits. As the bifurcation parameter is varied the branch of oscillatory solutions loses stability. This is due to a fold bifurcation, giving rise to regions in the parameter space where two different oscillatory solutions are possible for the same parameter values.

TABLE OF CONTENTS

LIST OF FIGURES

CHAPTER 1

Introduction

There would not be a field of science, from anthropology to zoology that does not use mathematical modelling techniques as an aid to research. In many cases the overall aim of the research is to produce a model that simulates a physical system, such as a meteorological model to predict the weather. This trend has arisen out of the computing revolution, owing largely to the fact that although we have always been able to make complex models, we can now solve them, albeit numerically. It is true that numerical techniques have been around for a long time but the possibility of using them to solve complex systems of differential equations would be time consuming even for an accomplished mathematician. With readily available mathematical software run on reasonably inexpensive computers researchers with only a basic knowledge of numerical analysis can nevertheless test their models.

The aim of mathematical modelling is to create a mathematical representation of a physical system, based on information provided by science about the system. As developers of a model we have two important aims. We need to show that the model is accurate, in that it resembles the actual situation in terms of its outputs. We also wish to know that our model is the simplest possible. By this we mean that the model could not be simplified further without changing the qualitative behaviour of any solutions for the system. It should be noted that when we test a model, our goal is to determine the qualitative behaviour of the solutions it provides. We cannot solve a complex system of equations for all cases. Instead we want to be able to make long term forecasts about the behaviour of the system they represent. In general then, we look for the types of solutions that are of use in practical applications. Another important consideration is to test the system of equations in a variety of situations that will give information about how the qualitative behaviour of the solutions depends on any parameters involved in the equations. In this way we can build upon the model to increase its complexity by introducing new terms or changing the form of existing terms. In the case of dynamical systems we usually generate a system of differential equations. The analysis of such a system of equations is independent of the specific application from which the equations were derived. How we do this is the domain of Dynamical Systems Theory. This is a rich body of knowledge, and may be found in texts such as Guckenheimer and Holmes (1983)

A dynamical system is generally defined as a rule that defines a subject's position in ambient space over time. Any continuous time model generated from this type of system will be in the form of a set of differential equations. We can then employ Dynamical Systems Theory, which builds on the well understood Linear Theory, to help us determine the qualitative behaviour of the solutions to this type of model. It should be noted here that by qualitative behaviour we mean looking at the form of the solutions in a parameter space. If we think of a system as an input-output mechanism then it is clear that it is not practical to look at the solutions for the possible range of all inputs.

Instead, we satisfy ourselves by examining inputs of practical importance. We are particularly interested in whether or not a solution will go to a steady-state over time or perhaps become chaotic in a certain region. We may also concern ourselves with oscillatory solutions which deal with finding systems where the dependent variables naturally oscillate over time. Another concern is bifurcation analysis which deals with how the qualitative behaviour of a solution changes abruptly when a parameter value is changed only slightly. Another important consideration is stability analysis. Here we investigate to see whether the solutions are stable or unstable with respect to small changes. Dynamical Systems theory has formulated many important results regarding the stability of solutions as well as generating many techniques with which to analyse a system. It has also given us a way of understanding the use of parameters to observe changes in equations which is of course of great practical benefit.

We now describe a dynamical systems theory approach to a general problem.
If we start with a system governed by the equations

$$\frac{dx_i}{dt} = f_i(x),\ i = 1,...,n,\ x \in \Re^n, \qquad (1.1)$$

generally we cannot solve this system algebraically. Instead we look for qualitative properties of a solution. This gives an overall picture of the behaviour of the system over time.

As previously mentioned, a primary consideration in dynamical systems theory is the existence of steady-state solutions. We are interested in whether the system has solutions which are independent of time. This is determined by finding solutions to the equation

$$f_i(x) = 0,\ i = 1,...,n\ . \qquad (1.2)$$

The solution x does not change over time. Solving the system (1.2) for x will give possible steady-states in terms of the parameters. Another consideration then is whether the steady-states are locally stable. This is equivalent to asking whether, for some steady state solution x^*, a nearby solution $x(t)$ with $x(0) = x^* + \varepsilon$ converges to x^* as t increases. The common approach to determining stability of an equilibrium point is to linearize the general system about the point by introducing a small perturbation of the form

$$x_i = x_{i0} + \varepsilon x_{i1} + O(\varepsilon^2)\ . \qquad (1.3)$$

Here ε represents the magnitude of the perturbation from the steady-state. This gives rise to the linearized system of equations,

$$\frac{dx}{dt} = Ax \qquad (1.4)$$

for the perturbed quantities. The matrix A in equation (1.4) contains the derivatives $\partial f_i / \partial x_j, i, j = 1,...,n$, evaluated at the equilibrium point. Typically in a dynamical system drawn from a physical model, the parameters will have known values and so we can evaluate A, and thus find the eigenvalues which in turn determine the stability of the steady-state.

We will now look at this situation for the two dimensional case. In two dimensions it is possible to observe the evolution, in time, of the solutions in the phase-plane. If we consider the general equations of the form,

$$dx/dt = f(x,y), \quad dy/dt = g(x,y) \tag{1.5}$$

there is a unique curve through any point (x_0, y_0) except for the singular points (x_s, y_s) where $f(x_s, y_s) = g(x_s y_s) = 0$. We can make a transformation so that (1.5) has a singular point at the origin $(0,0)$. If the equations f and g are analytic at the origin then we can expand them in a Taylor series expansion retaining only the linear terms, which leaves us with

$$dx/dt = ax + by, \quad dy/dt = cx + dy. \tag{1.6}$$

This is the two-dimensional equivalent of equation (1.4), with

$$A = \begin{vmatrix} a & b \\ c & d \end{vmatrix} = \begin{vmatrix} f_x & f_y \\ g_x & g_y \end{vmatrix}_{(0,0)}. \tag{1.7}$$

The eigenvalues λ_1, λ_2 of this (Jacobian) matrix are found by evaluating the characteristic polynomial and as such are solutions to the equation

$$\mathrm{Det}|A - \lambda I| = \mathrm{Det}\begin{vmatrix} (a-\lambda) & b \\ c & (d-\lambda) \end{vmatrix} = 0. \tag{1.8}$$

Solutions of (1.6) are of the form

$$\begin{pmatrix} x \\ y \end{pmatrix} = c_1 v_1 e^{\lambda_1 t} + c_2 v_2 e^{\lambda_2 t} \tag{1.9}$$

Where c_1, c_2 are arbitrary constants and v_1, v_2 are the eigenvectors of A, corresponding to λ_1, λ_2 respectively.

The solutions have different behaviours depending on the qualitative values of the eigenvalues. The six common forms can be viewed in the phase-plane for (x, y). They are displayed in Figure 1.

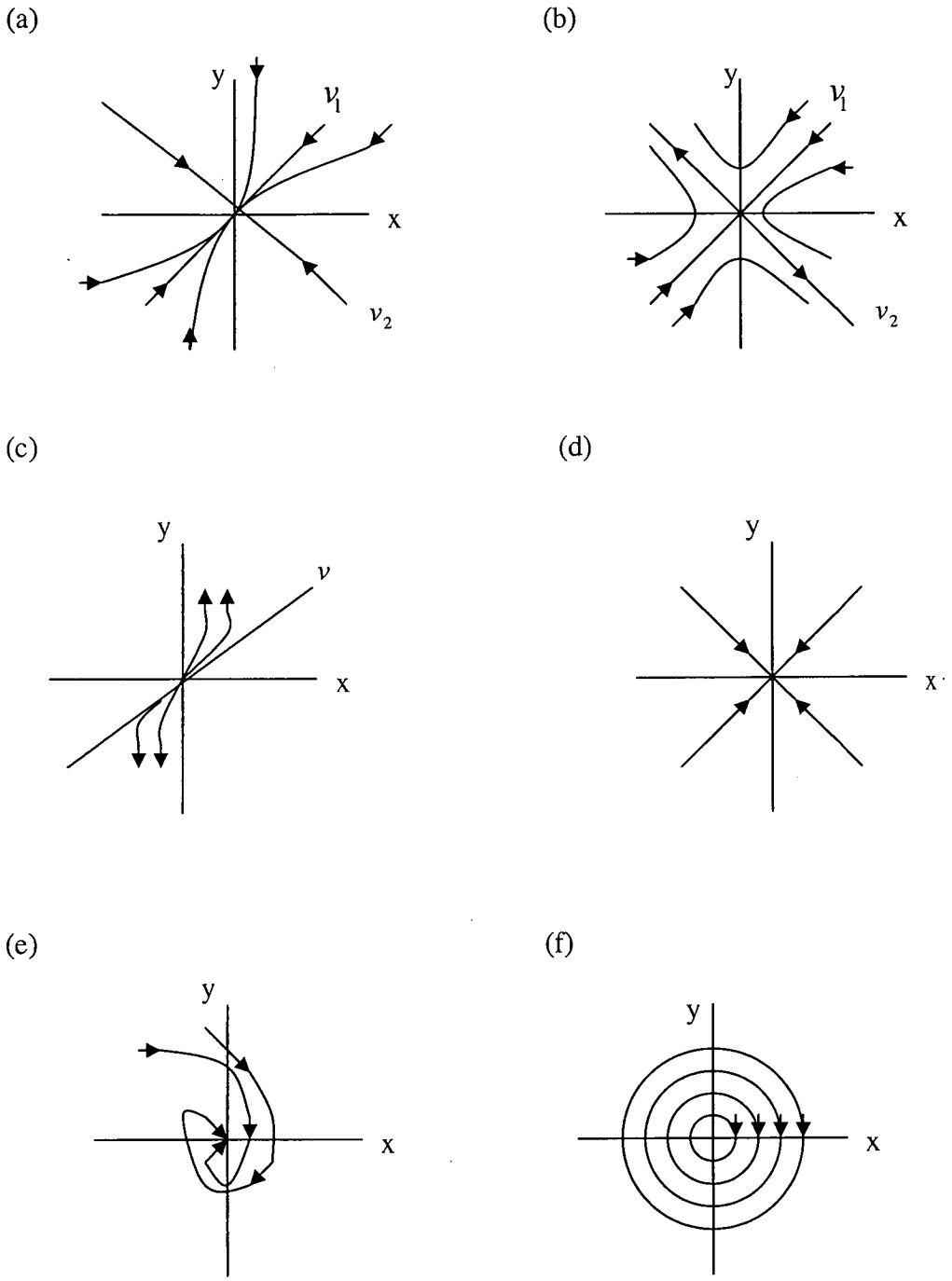

Figure 1.1 six typical basic linear singularities. The direction of the arrow shows whether the solution branch is moving towards or away from the singularity at (0,0). (a): node: can be stable or unstable. (b) saddle point: which is always unstable.(c) Node (type II): these can be stable or unstable. (d) star: can be stable or unstable (e) spiral: can be stable or unstable. (f) centre: neutrally stable

If λ_1, λ_2 are real and distinct, then if they have the same sign we have Fig 1.1(a) a node which will be stable if the sign of the eigenvalues is negative, otherwise the node will be unstable. If they have different signs then we have a saddle point as shown in Fig 1.1(b). If $\lambda_1 = \lambda_2$ then in general the solution will contain terms like $te^{\lambda t}$ and as there is only one eigenvector along which the solutions tend to (0,0), this critical point can be either stable or unstable depending on the sign of λ. This degenerate situation is shown in Fig 1.1 (c). If there is no term like $te^{\lambda t}$, as shown in Fig 1.1(d), we have a node (type 2) which once again may be stable or unstable dependent on the sign of λ. If λ_1, λ_2 are complex and they have the form $\alpha \pm i\beta, \beta \neq 0$, then we have a stable focus if $\alpha < 0$ as shown in Fig 1.1(e). If $\alpha > 0$ the focus will be unstable. If $\alpha = 0$ then we have a centre. Centres are neutrally stable, in the sense that any perturbation from the orbit doesn't return to it, but instead forms a separate orbit about the critical point. This is shown in Fig 1.1(f).

Thus the form of the solution depends on the parameters *a, b, c* and *d* in equation (1.7). If we have a situation where a focus solution cannot leave a bounded set nor can it reach its critical point, then we must have a limit cycle in the phase plane by the Poincare-Bendixson theorem (Murray 1989). Limit cycles are representative of self-sustained oscillatory behaviour in the solutions. They may arise through bifurcation at a parameter value at which the linearised solution would find a centre. A bifurcation refers to the case where the number of steady states in a system changes or there is a change in stability of an existing steady state, as a parameter is changed. A bifurcation generally occurs when the real part of an eigenvalues at an equilibrium point passes through zero as a parameter is varied, therefore changing the stability of the point. If a pair of eigenvalues becomes purely imaginary at this point we have a Hopf bifurcation.

Scientists are interested in oscillatory nature of solutions because they are a feature of biological systems, as shown by Shertzer *et al* (2002). Studies show that in a two-dimensional predator prey system over time predator numbers may increase and as such prey numbers decrease. As prey numbers decrease so may predator numbers. This gives prey an opportunity to recover and so their numbers increase again, followed by an increase in the numbers of predators, and so on. This is an example of an oscillatory solution and we have already outlined how a dynamical systems approach can be used to predict conditions under which oscillatory solutions may form. In addition, we can predict whether the solution is stable or not. Commonly we use the Hopf bifurcation to predict the existence of limit cycles. Generally, we will vary one parameter and try to locate a critical value at which a Hopf bifurcation occurs. For example, in the previous phase plane analysis we know that the eigenvalues are given by (1.8) as,

$$\lambda_1, \lambda_2 = \frac{1}{2}\left((a+d) \pm \sqrt{(a+d)^2 - 4(ad-bc)}\right). \qquad (1.10)$$

A necessary, but not sufficient condition, for equation (1.10) to give a Hopf point would be the following

$$a = -d \quad \text{and} \quad a^2 + bc < 0 \,. \qquad (1.11)$$

Thus the eigenvalues become $\lambda_1, \lambda_2 = \pm i\sqrt{-a^2 - bc}$, so that at the possible Hopf bifurcation point (1.11), a limit cycle may be born with oscillatory frequency $2\pi / \sqrt{-a^2 - bc}$. In a practical situation, we might therefore vary the parameter a and observe the solutions as we pass through the Hopf point (1.11), keeping the other parameters constant.

Limit cycles are periodic solutions with non zero amplitude. Nearby solutions are bounded by these structures in that they either converge to them or diverge from them. We can determine whether the limit cycles are stable or not using Floquet theory, which deals with periodic solutions and provides methods to test if a linear approximation to a limit cycle converges to the limit cycle. Floquet theory can also be used to show if there is period doubling in the solution, which can be a route to chaos. Shertzer *et al* (2002) have found limit cycle behaviour in a laboratory using just two species. We therefore know these structures exist in nature. However, they may be obscured in a far more complex ecosystem. Nonetheless, they will still have an effect on the overall dynamics of the larger system. We look more closely at the theory behind limit cycle stability in chapter 3 of this thesis.

Oscillatory solutions are, of course, not necessarily periodic. In non-periodic solutions we look for such qualitative behaviour as quasi periodicity and chaos. Quasi-periodicity occurs when a solution appears to form non-repeating patterns, although it turns out that the solution is actually made up of two different frequencies with a ratio that is an irrational number. The Ruelle-Takens-Newhouse theorem predicts that Quasi-periodicity can be a route to chaos (see the discussion in Thompson and Stewart 1989, page 196). This can occur if the quasi-periodic solution itself undergoes a (secondary) Hopf bifurcation to produce a third frequency component that is an irrational multiple of the previous two. Once the third frequency appears in the solution, then the solution is structurally unstable and will become chaotic. Once again, this behaviour is not just a theoretical construct, as Jansen (2001) found quasi-periodicity within a two dimensional predator-prey system which was dependant on migration rates of the predator.

In this thesis we are investigating a model taken from a paper by Lewi Stone (1990) describing a five dimensional food web. The paper deals with predator-prey interactions, which have been of great interest both to practical and theoretical biologists over a long period of time. In particular, naturally occurring oscillations of populations in time have been studied in a variety of practical situations (Murray 1989). Famous models, such as the Lotka-Volterra system, have been developed to explain theoretically the source of these oscillations in fish populations, and such behaviour is also exhibited in Phytoplankton (Edwards et al 1999). Oscillations may be possible in the unforced case dependant on parameter values. Huppert et al (2004) found for example that the rate of Zooplankton growth has an effect on Phytoplankton blooms. Seasonally related phenomena (Truscott et al 1994) have been observed in Phytoplankton, which suggests that seasonal forcing of populations may also be of importance in modelling. In fact, Edwards (2001) found that "seasonal forcing of some of the parameters may be taking the system from a region of parameter space where the unforced system would be attracted to a stable steady state, into a region during the summer months where the unforced system would exhibit stable oscillatory behavior".

Stone (1990) studied a two level trophic web found in the Southern Oceans. In particular he sought to explain the paradoxical nature of the interaction between Phytoplankton and Bacteria that form part of the system. Both species compete for the same limiting inorganic nutrients. When these nutrients are scarce, the Phytoplankton release Extracellular Organic Carbon (EOC) which is used by the Bacteria. In essence, the Phytoplankton directly promotes the survival of a competitor. This is intuitively at odds with the nature of competition. To explain this phenomenon, Stone (1990) refers to the idea that ecologists commonly use a reductionist approach to view interactions. Behaviour is deduced from the interactions between organisms in isolation rather than as one of many interactions in a wider community. For example, if Phytoplankton are disadvantaged by the presence of Bacteria which in turn are predated by Protozoa, then it is conceivable that Phytoplankton, by stimulating the growth of Bacteria may be also stimulating the growth of the Protozoa which graze on them. This may prove advantageous to the Phytoplankton. In fact this may be a case of the Paradox of Enrichment (Kirk 1998) whereby adding more prey results in population cycles that increase in amplitude. Gross et al (2004) showed that the dynamics of a general predator prey system can be either stabilized or destabilized by enriching the prey, dependant on the form of the interaction function used.

Much research has been performed on the stability of populations in biological models, focussing on how populations are drawn to attractors such as limit cycles or steady-states, or if and when extinction occurs. Shertzer et al (2002) found that a simple mechanistic model of a four species predator-prey interaction agreed with data collected in a chemostat experiment. The model predicted limit cycle, steady-states and extinction behaviour present in the chemostat, although the results differed on the prediction of period and phase. The model was improved to include the ability of prey to evolve defence mechanisms, and was found to be accurate in all respects. Hutchison (1961) theorised that Plankton communities cannot come to equilibrium but continue to develop to oscillatory solutions or chaos owing to all the external effects they are subject to as their environment changes. Scheffer et al (2003) found that "various competition and predation models suggest that even in homogeneous and constant environments plankton will never settle to equilibrium." This was also found in experimentation and that chaos quite often resulted in low dimensional systems. This has the outcome of making long term predictions about such systems impossible. However, Verschoor et al (2004) subsequently "showed experimentally that bi-and tri-trophic food chains with induced defences approached a stable equilibrium without any oscillatory tendency, while those without defences in the algae showed high-amplitude population". Van der Stap et al (2008), showed for tri-trophic model that population stability of phytoplankton occurred in a tri-trophic model when the phytoplankton had a defence mechanism which affected the uptake interaction of the Zooplankton. We can conclude from these studies that the differences regarding population stability are a result of the conditions under which these results were obtained. By this we mean that if the number of species present and environmental variables differs from experiment to experiment, then so do the results.

Other dynamical structures such as quasi-periodicity have also been found in higher dimension food webs similar to the one being examined here. Ruan *et al* (2001)

examined a three dimensional model involving Zooplankton, Phytoplankton and nutrients in limited supply. Modelling nutrients with both instantaneous and delayed recycling they found that the equilibrium point loses stability when a critical value is reached in nutrient levels and passes via a Hopf-bifurcation into a limit cycle. On the other hand, Wang et al (2005) found in a three dimensional food web with non-linear nutrient dependence there was limit cycle behaviour, quasi-periodicity and chaos.

In this thesis we will use the ideas discussed but in greater detail to examine the model described by Stone (1990). This model describes a five dimensional food web. We will begin by formulating a simple model involving just the straightforward Lotka-Volterra interaction. This way we can get an idea of the dynamics of the simplified system. In this first formulation of the model we will look at the system under the assumption that nutrients are in plentiful supply. We will analyse the model using dynamical systems theory to look for both steady state and oscillatory solutions. We will then seek to determine whether oscillatory solutions can arise as the result of a Hopf bifurcation.

In the next phase of analysing the system under the assumption that nutrients are in plentiful supply we will look at periodic forcing. This corresponds to looking at diurnal effects on the system. This is achieved by changing the form of the interaction function for one of the species. In this case we look for resonance in the linearised system. This may be seen as analogous to phenomena such as algal blooms in nature.

In the third chapter we allow nutrient concentration to vary and thus increase the complexity of the model. Once again using dynamical systems theory we will analyse the model. In this case we are looking for behaviour such as steady-states and oscillatory solutions. We are looking for the presence of a Hopf bifurcation or in fact any bifurcation point that alters the dynamics of the system. We found limit cycles and, using Floquet theory, we determined that their stability changed as we moved along a solution branch. We found no evidence of period doubling in the solutions.

In the last chapter we provide an overall summary of the work undertaken in this thesis, along with some indications of possible future research.

CHAPTER 2

Simple Model Including Forcing Term

In this chapter, we present a detailed analysis of Stones' (1990) model of phytoplankton and bacteria interaction, with a two level trophic web in which protozoa and zooplankton are also included. Ideas from the theory of dynamical systems (see Murray 1989, Edelstein-Keshet 1988 for more discussion) are used here to investigate the stability of steady-state populations and the possibility of self sustained oscillations. As was mentioned in the introductory chapter, we do not consider the nutrient term (in Figure 2.1.) in our first analysis of the system. This can be considered equivalent to assuming the nutrients to be in ample supply and therefore any loss, or gain, to nutrient mass does not affect the system in any way. In this way we can remove the nutrients term from the equations governing the system. This will give us important information about the behaviour of the system under this condition, since although Stone (1990) sought to understand the behaviour of the model when nutrients were limited, to understand the system fully and see the overall effects of nutrients, it is important to understand this simplified system.

In addition to looking at the system without the nutrient term, we also allow the growth rate of bacteria to vary sinusoidally, as a model for seasonal (or diurnal) fluctuations. This can have the effect of making the solutions oscillatory with the same period as the forcing frequency, or if the solutions are already oscillatory then the combination with the forcing frequency may present itself in the form of resonant peaks in the solutions. As it stands the model is non-linear, and so we find a complicated resonance pattern in the results, and suggest even the possible presence of quasi-periodicity and chaos for certain parameter values.

The model is presented in Section 2.1 and for convenience scaled (non-dimensional) populations and rates are introduced. In Section 2.2 we provide an analysis of the model. Section 2.3 presents a linearized analysis of the seasonally-forced model in which we assume small amplitude for the forcing term. Two (primary) resonance peaks are shown to be present. Numerical results are then found, in section 2.4, for the non-linear model. Multiple resonance peaks and even possible quasi-periodic and chaotic behaviours are found. This chapter concludes with a discussion in Section 2.5.

2. 1 The Mathematical Model

We consider the two-level trophic system illustrated in Figure 2.1, taken from the model proposed by Stone (1990). There are five interacting compartments, namely Bacteria (B), Phytoplankton (P), Zooplankton (Z), Protozoa (R) and Nutrients (N) and these are indicated in the diagram.

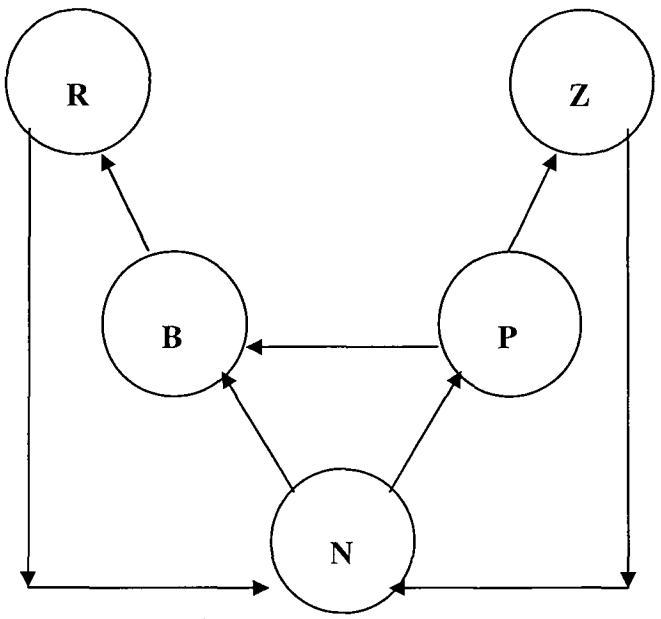

Fig. 2.1 Stone's Compartmental model showing interaction between components. The direction of the arrows indicates a direct positive influence by one component on another. Here R,B,N,P,Z represent protozoa, bacteria, nutrients, phytoplankton , zooplankton respectively. The effect of nutrients N is ignored in the present study.

The arrows show positive interaction between components in the model, where for example R benefits from the presence of B but B is negatively affected by the presence of R. Fig 2.1 contains two predator prey systems, one for the bacteria and protozoa and one for the phytoplankton and zooplankton. In simplest terms population mechanics is governed by the idea that a species numbers changes according to the following rule,

Rate of Change of a Population = Reproduction Rate – Mortality Rate + Migration.

In this thesis, migration is not considered; instead we consider the system closed. We represent the predator prey relationship in the form of a Lotka-Volterra model, which in the general two dimensional case can be given by

$$\frac{dP_1}{dt} = P_1(a - bP_2) \quad , \quad \frac{dP_2}{dt} = P_2(cP_1 - d) .$$

Here P_1 is the population of prey and P_2 is the population of predator, and a, b, c and d are positive constants. The reproductive rate of the prey, given by the term aP_1, is

proportional to the number of prey present. This encapsulates the idea that the prey population will naturally increase by a percentage of its current population. Furthermore this type of model assumes that without predators, $P_2 = 0$, the prey growth, $dP_1 / dt = aP_1$, is exponential. Predator reproduction, given by the term cP_1P_2, is proportional to the predation rate, which is modelled by this interaction term that represents the probability of predator and prey being in the same location at the same time. Clearly, in the absence of prey, $P_1 = 0$, the predator population, $dP_2 / dt = -dP_2$, dies off. Similarly the mortality rate of the prey, $-bP_1P_2$, is likewise proportional to their predation rate. The mortality rate of the predator, $-dP_2$, is proportional only to the number of predators present, so we expect a percentage of the predators will die off within a given interval of time.

As previously mentioned we will not be considering migration in this thesis. Stone likewise did not consider this in his paper and the effect is therefore not present in the model detailed in Fig 2.1. Although migration is a factor worth considering there are many different levels of complexity or alternate methods used to model population dynamics (see Murray (1989) for further discussion). We can for example, represent birth rate as a delay term where gestation period and reproductive maturity of an individual are taken into account. A delay term may determine the current growth rate of a species by examining the growth rates of the species at earlier times with respect to the then populations. The real point to be considered here is that although there are more or less realistic models available, models at all levels of complexity will furnish important results about the dynamics of a system.

In this chapter we consider the case in which the nutrient concentration N is inexhaustible, and therefore not subject to change. With this in mind we now look to construct the governing equations for Stone's (1990) system. Following the same approach as outlined in the classical Lotka-Volterra system, the interaction in Figure 2.1 gives rise to the system of four ordinary differential equations

$$\begin{aligned} dB/dt &= r_b B - r_r RB + r_i PB \\ dP/dt &= r_p P - r_z PZ - r_i BP \\ dZ/dt &= r_z PZ - d_z Z \\ dR/dt &= r_r RB - d_r R \end{aligned} \qquad (2.1)$$

for the time-dependant behaviour of the populations of the four species. In Stone's (1990) original model, the interaction between bacteria and phytoplankton was described as an example of commensalism, in which B benefited from P, but without cost to phytoplankton P. Here, however, we have assumed a simpler situation that interactions between any two compartments illustrated in Figure 2.1 result in a gain to one and a loss to the other. In a biological setting this would assume the relationship to

be more akin to parasitism than commensalism, which is modelled by a negative interaction term in the rate of change equation for the host and a positive term in the equation for the parasite. We can see from these equations that in the absence of a nutrients term, the four equations (2.1) look like two predator-prey systems connected by what looks like a predator birth rate term in the rate of change equation for bacteria and a prey mortality rate term in the rate of change of phytoplankton equation. In this system (2.1), the symbol r_b denotes the growth rate of bacteria, and r_p is the reproduction rate for phytoplankton. The three quantities r_r, r_i and r_z are the (second order) interaction rates between protozoa and bacteria, bacteria and phytoplankton and zooplankton and phytoplankton respectively. The remaining terms d_z and d_r are the mortality rates of zooplankton and protozoa. All these quantities are positive.

In the present investigation, we undertake an analysis of the dynamical behaviour of the system (2.1) in the unforced case in which all the parameters are constants. Of particular interest are conditions necessary for a solution to exhibit oscillatory behaviour. If possible, we also wish to identify those situations in which a limit cycle may be born by means of a Hopf Bifurcation, which occur when a non-linear self-sustained oscillation appears directly from a steady-state population as a parameter is varied (Murray 1989).

We are also interested in the effect of subjecting the system (2.1) to external periodic forcing, arising physically from seasonal or daily variations in the environment. This is achieved mathematically by representing the reproduction rate for bacteria r_b in the form

$$r_b = r_{b0} + r_{b1}\cos(\omega t). \qquad (2.2)$$

Here, r_{b0} is the average breeding rate and r_{b1} is the forcing amplitude. The constant ω is the frequency of the seasonal forcing, and has units day^{-1}. As indicated by Edwards and Brindley (1999), this term indicates that bacteria are more likely to reproduce in daylight.

The original system of equations (2.1) is now re-cast in terms of dimensionless variables. This is done in order to simplify the model, particularly as it results in fewer dimensionless groupings of parameters, rather than isolated model parameters that must be varied individually in order to analyse the model fully. To non-dimensionalise the equations we consider the bacteria population in the form,

$$B = B_s \hat{B} \qquad (2.3)$$

where $\hat{B}$ is a dimensionless quantity and the B_s represents a scale that will be chosen later. Scalings similar to (2.3) are likewise made to the other variables P, R, and Z in equations (2.1). Time is also scaled in the same way. We substitute this form into equations (2.1) so that the first equation looks like,

$$B_s d\hat{B}/t_s d\hat{t} = r_b B_s \hat{B} - r_r R_s B_s \hat{R}\hat{B} + r_i B_s P_s \hat{B}\hat{P}. \qquad (2.4)$$

We made use of the chain rule here $dB/dt = B_s(d\hat{B}/d\hat{t}).(d\hat{t}/dt)$ and also the fact that $\hat{t}/t = 1/t_s$. Once we have divided both sides of (2.4) by B_s/t_s this equation becomes

$$d\hat{B}/d\hat{t} = r_b t_s \hat{B} - r_r R_s t_s \hat{R}\hat{B} + r_i P_s t_s \hat{B}\hat{P} \qquad (2.5)$$

The above equation has three dimensionless parameter grouping, $r_b t_s$, $r_r R_s t_s$ and $r_i P_s t_s$.

Once we have determined all these groupings by applying this same procedure to the remaining three equations in (2.1), we can choose suitable scales to reduce the number of parameters. The full set of parameter groupings are given by

$$\begin{array}{lll} r_b t_s\,, & r_r R_s t_s\,, & r_i P_s t_s \\ r_p t_s\,, & r_z Z_s t_s\,, & r_i B_s t_s \\ r_z P_s t_s\,, & t_s d_z & \\ r_r B_s t_s\,, & t_s d_r & \end{array} \qquad (2.6)$$

We now use look to make choices for some of the dimensional quantities so as to reduce the number of parameter grouping in (2.6) by reducing their values to unity. The time scale was chosen as $t_s = 1/r_p$ which is a time scale linked roughly to the lifecycle of the phytoplankton. We also assume that all populations are roughly the same order of magnitude so that $B_s = P_s = Z_s = R_s$ and that all four populations (B, P, Z, R) are scaled with respect to the quantity r_p/r_r which is a naturally occurring measure of population coming from equations (2.1). In these non-dimensional variables, equations (2.1) become

$$\begin{aligned} \mathrm{dB/dt} &= \beta \mathrm{B} - \mathrm{RB} + \eta \mathrm{PB} \\ \mathrm{dP/dt} &= \mathrm{P} - \alpha \mathrm{PZ} - \eta \mathrm{PB} \\ \mathrm{dZ/dt} &= \alpha \mathrm{PZ} - \delta \mathrm{Z} \\ \mathrm{dR/dt} &= \mathrm{RB} - \gamma \mathrm{R}. \end{aligned} \qquad (2.7)$$

There are now only four dimensionless parameter groupings in the system (2.7). These are

$$\alpha = \mathrm{r}_z/\mathrm{r}_r,\ \gamma = \mathrm{d}_r/\mathrm{r}_p,\ \delta = \mathrm{d}_z/\mathrm{r}_p,\ \eta = \mathrm{r}_i/\mathrm{r}_r. \qquad (2.8)$$

The first of these parameters, α, represents the reproduction rate of phytoplankton. The second, γ, corresponds to the mortality rate of the protozoa. The third parameter, δ, is the mortality rate of the zooplankton and the fourth quantity, η, is the relative rate of interaction between the Bacteria and Phytoplankton. All four parameters are constants, and in addition there is a time-dependant reproduction rate for bacteria

$$\beta = \beta_0 + \beta_1 \cos \Omega t \ , \qquad (2.9)$$

from equation (2.2). This relation (2.9) introduces three additional non-dimensional parameters

$$\beta_0 = r_{b0} / r_p \ , \ \beta_1 = r_{b1} / r_p \ , \ \Omega = \omega / r_p \ . \qquad (2.10)$$

The first of these is the steady-state reproduction rate for bacteria. The second parameter β_1 is the seasonal forcing amplitude for that reproduction rate, and the final parameter Ω is its forcing frequency relative to the time scale for natural bacterial growth. Thus the model is fully described by the set of seven constants in equations (2.8) and (2.10).

2.2. Analysis of the Model

This section begins by considering the dynamics of the system (2.7) without seasonal forcing, so that $\beta_1 = 0$.

2.2.1 Steady-state Populations without seasonal forcing

Steady states are solutions (B, P, Z, R) which satisfy

$$dB/dt = \ dP/dt = \ dZ/dt = dR/dt = \ 0.$$

There are five separate equilibria for the non-dimensional model system (2.7). These may be determined to be

$$\begin{aligned}
&(Beq, Peq, Zeq, Req) \ = \ (0, 0, 0, 0) \\
&(Beq, Peq, Zeq, Req) \ = \ (1/\eta, -\beta/\eta, 0, 0) \\
&(Beq, Peq, Zeq, Req) \ = \ (\gamma, 0, 0, \beta) \\
&(Beq, Peq, Zeq, Req) \ = \ (0, \delta/\alpha, 1/\alpha, 0), \\
&(Beq, Peq, Zeq, Req) = \ (\gamma, \delta/\alpha, (1-\delta\gamma)/\alpha, \beta + \eta\delta/\alpha). \qquad (2.11)
\end{aligned}$$

The first steady state in equation (2.11) represents the case where all four species become extinct. In the second steady state, two of the species survive and the population of one of these is negative and thus not physically meaningful. For the third and fourth steady states, two of the species survive and two again become extinct. The surviving species in these two states form an independent predator prey coupling, each involving two species only, and correspond closely to the famous Lotka-Volterra system in

Murray (1989). The fifth and final steady state in (2.11) is potentially of most interest here, as it represents the situation when all four species survive.

2.2.2 Stability of Steady-states

When the time-independent populations are close to any of the five steady states in equations (2.11), the small-amplitude behaviour may be determined by linearization, in the form

$$\begin{aligned} B(t) &= Beq + \varepsilon B_1 + O(\varepsilon^2), \\ P(t) &= Peq + \varepsilon P_1 + O(\varepsilon^2) \\ Z(t) &= Zeq + \varepsilon Z_1 + O(\varepsilon^2) \\ R(t) &= Req + \varepsilon R_1 + O(\varepsilon^2). \end{aligned} \tag{2.12}$$

The constant ε is supposed to be small, and represents a measure of how close the system is to one of its steady states (2.11). The linearized system near an equilibrium point is determined by substituting these forms (2.12) into the governing equations (2.7). We will show this for the first equation in (2.7) which becomes,

$$\begin{aligned} dB_{eq}/dt + \varepsilon dB_1/dt = \beta(B_{eq} + \varepsilon B_1) - (R_{eq}B_{eq} + \varepsilon(R_{eq}B_1 + B_{eq}R_1)) \\ + \eta(B_{eq}P_{eq} + \varepsilon(P_{eq}B_1 + B_{eq}P_1)) + O(\varepsilon^2). \end{aligned}$$

We know that $dB_{eq}/dt = 0$ and that $\beta B_{eq} - B_{eq}R_{eq} + \eta B_{eq}P_{eq} = 0$ so we can remove these terms from the above equation. Retaining terms up to order ε, the linear approximation for bacteria is given by

$$dB_1/dt = \beta B_1 - (R_{eq}B_1 + B_{eq}R_1) + \eta(B_{eq}P_1 + P_{eq}B_1)$$

If we do this for all the other equations in (2.7) this results in the linear matrix system

$$\mathrm{d/dt}\begin{bmatrix} B_1 \\ P_1 \\ Z_1 \\ R_1 \end{bmatrix} = \begin{bmatrix} J_{11} & \eta Beq & 0 & -Beq \\ -\eta Peq & J_{22} & -\alpha Peq & 0 \\ 0 & \alpha Zeq & -\alpha\delta Peq & 0 \\ Req & 0 & 0 & J_{44} \end{bmatrix}\begin{bmatrix} B_1 \\ P_1 \\ Z_1 \\ R_1 \end{bmatrix}, \tag{2.13}$$

where, for convenience, we have defined intermediate quantities

$$J_{11} = \beta_0 - R_{eq} + \eta P_{eq}$$

$$J_{22} = 1 - \alpha Z_{eq} - \eta B_{eq}$$
$$J_{44} = B_{eq} - \gamma .$$

We substitute, in turn, each equilibrium point into (2.13) to determine the eigenvalues of the constant 4X4 constant (Jacobian) matrix for that steady-state. In each case, the four eigenvalues so obtained determine the behaviour of the linearized system near the corresponding equilibrium point.

From this analysis it may be determined that the first point (0, 0, 0, 0) in (2.11) is a saddle, with eigenvalues given $\beta_0, 1, -\delta, \gamma$. Similarly, the second point $(1/\eta, -\beta_0/\eta, 0, 0)$ is also a saddle, and its eigenvalues are $1/\eta - \gamma, -\alpha\beta_0/\eta - \delta, \pm\beta_0$. The third point ($\gamma$, 0, 0, β_0) in (2.11) has eigenvalues given by $1 - \eta\gamma, -\delta, \pm i\sqrt{\beta_0\gamma}$, and the point (0, δ/α, $1/\alpha$, 0) has eigenvalues given by $\beta_0 + \eta\delta/\alpha, -\gamma, \pm i\sqrt{\delta}$. Both these points are essentially saddles, in the sense that they combine stable behaviour (negative eigenvalues) with unstable (positive eigenvalues). However, they both possess a pair of purely imaginary eigenvalues, and this gives them an oscillatory behaviour in some plane passing through the equilibrium point in the phase space. In this regard these two equilibria could give similar oscillatory behaviour to the famous Lotka-Volterra system, in which a non-linear centre occurs (Murray 1989).

The steady-state of most practical interest is the fifth point (γ, δ/α, $(1-\delta\gamma)/\alpha$, $\beta_0 + \eta\delta/\alpha$) in the system (2.11), at which none of the populations disappear. The eigenvalues λ for this case can be found from the equation

$$\det \begin{bmatrix} -\lambda & \eta\gamma & 0 & -\gamma \\ -\eta\delta/\alpha & -\lambda & -\delta & 0 \\ 0 & 1-\eta\gamma & -\lambda & 0 \\ \beta+\eta\delta/\alpha & 0 & 0 & -\lambda \end{bmatrix} = 0$$

This may be expanded to give the quartic equation

$$\lambda^4 + \quad T\lambda^2 + \quad D \quad = \quad 0 \qquad (2.14)$$

In which it is convenient to define the quantities

$$T = \gamma(\beta + \eta\delta/\alpha) + \delta(1 - \eta\gamma) + \eta^2\gamma\delta/\alpha \qquad (2.15)$$
$$D = \gamma\delta(1-\eta\gamma)(\beta + \eta\delta/\alpha).$$

The quartic equation (2.14) for the eigenvalues λ has the solution

$$\lambda^2 = \frac{-T \pm \sqrt{T^2 - 4D}}{2} \qquad (2.16)$$

There are four eigenvalues λ as solutions to (2.16). If any two of them form a complex conjugate pair that crosses the imaginary axis as a parameter is varied, a Hopf bifurcation is generated (see Guckenheimer and Holmes 1983, page 151). Thus a necessary condition for limit-cycle generation in this way is that the real part of a complex conjugate pair changes sign. It is convenient to introduce the notation

$$X = \beta + \eta\delta/\alpha, \qquad Y = 1 - \eta\gamma, \qquad S = \eta^2\gamma\delta/\alpha \qquad (2.17)$$

in terms of which the quantities in equation (2.15) take the simpler forms

$$T = \gamma X + \delta Y + S \ , D = \gamma\delta XY \ . \qquad (2.18)$$

We observe that D > 0 in equation (2.18), since the parameter values given in Stone's (1990) paper show that $1 - \eta\gamma > 0$. For a Hopf bifurcation to occur, the real part of λ in equation (2.16) must change sign, and therefore firstly it must vanish at a particular parameter value (the Hopf bifurcation value), for non-zero imaginary part. A necessary condition for this to occur is therefore that

$$T > 0 \text{ and } T^2 - 4D > 0 \ . \qquad (2.19)$$

However, it follows from equations (2.17) and (2.19) that

$$T^2 - 4D = \gamma^2 X^2 + 2\gamma X(S - \delta Y) + (S + \delta Y)^2 \ . \qquad (2.20)$$

The right-hand side of equation (2.20) is an irreducibly positive quadratic in X, for all $Y > 0$. Thus the inequalities in (2.19) are satisfied for all $Y > 0$, so that the real part of λ in equation (2.16) cannot change sign, but is always zero. This shows that there cannot be a Hopf bifurcation in the system (2.7) for $\eta\gamma < 1$, which is the case of practical interest as indicated by Stone (1990).

Although the system has no Hopf Bifurcation it is clear from (2.19) and (2.16) that the eigenvalues for this steady-state are

$$\lambda = \pm i\sqrt{\frac{T \pm \sqrt{T^2 - 4D}}{2}} \qquad (2.21)$$

This means that the linearized system predicts a neutrally stable centre at this equilibrium, surrounded by concentric periodic orbits (see Medio and Lines 2001, page 40). This is, however, not necessarily an indication of the behaviour of the corresponding non-linear system (2.7), since the Hartman linearization theorem fails at a centre (see, Guckenheimer and Holmes, page 13), and additional information is needed in order to establish the behaviour of the non-linear system near the equilibrium.

Accordingly, we have examined the full system (2.7) numerically and have indeed observed non-linear centre behaviour in the unforced system.

2.3. External Forcing

Due to seasonal and diurnal influences, it is now assumed that the growth rate β for bacteria is not a constant, but varies with time as detailed in equation (2.9). We now consider that the seasonal forcing amplitude β_1 in (2.9) is a small parameter, and linearize about the fifth steady-state point in equation (2.11) using perturbation expansions of the form

$$\begin{aligned} B(t) &= Beq + \beta_1 B_1 + O(\beta_1^{\,2}) \\ P(t) &= Peq + \beta_1 P_1 + O(\beta_1^{\,2}) \\ Z(t) &= Zeq + \beta_1 Z_1 + O(\beta_1^{\,2}) \\ R(t) &= Req + \beta_1 R_1 + O(\beta_1^{\,2}). \end{aligned} \tag{2.22}$$

When equations (2.22) are substituted into the governing system (2.7) and (2.9), for the fifth equilibrium in (2.11), and the terms are retained to the first order in β_1, there results the linear system of forced equations

$$\begin{aligned} dB_1/dt &= \gamma \cos \Omega t - \gamma R_1 + \gamma \eta P_1 \\ d\,P_1/dt &= -\delta Z_1 - \frac{\eta \delta}{\alpha} B_1 \\ d\,Z_1/dt &= Y\,P_1 \\ d\,R_1/dt &= X\,B_1 . \end{aligned} \tag{2.23}$$

in which the two constants X and Y are as defined in equation (2.17).

It is known that periodic solutions to (2.23) are of the form

$$\begin{aligned} B_1(t) &= a_1 \cos \Omega t + b_1 \sin \Omega t \\ P_1(t) &= a_2 \cos \Omega t + b_2 \sin \Omega t \\ Z_1(t) &= a_3 \cos \Omega t + b_3 \sin \Omega t \\ R_1(t) &= a_4 \cos \Omega t + b_4 \sin \Omega t . \end{aligned} \tag{2.24}$$

After some algebra, the amplitude constants in equations (2.24) may be shown to be given by the relations

$$\begin{aligned} a_1 &= 0 & b_1 &= -(\Omega L)/(MX) \\ a_2 &= \Omega^2 \eta \delta \gamma / M & b_2 &= 0 \\ a_3 &= 0 & b_3 &= \Omega Y \eta \delta \gamma / M \end{aligned} \tag{2.25}$$

$$a_4 = L/M \qquad b_4 = 0$$

in which the quantities

$$L = -\alpha\gamma X(\Omega^2 - \delta Y)$$
$$\mathrm{M} = \alpha\Omega^4 + \Omega^2(-\alpha\gamma X - \alpha\delta Y - \eta^2\gamma\delta) + \gamma\delta\alpha XY \qquad (2.26)$$

have been defined for convenience. This linearized solution (2.24) breaks down whenever the amplitude constants in equations (2.25) fail to be defined. This is the point of primary resonance in the forced system. It occurs when M = 0 leading at once to the quartic equation

$$\Omega^4 - T\Omega^2 + \gamma\delta XY = 0 \qquad (2.27)$$

for the frequency Ω. The quantities T, X and Y are as defined in equations (2.15) and (2.17).

It follows from equation (2.27) that resonance will occur at the frequencies .

$$\Omega = \sqrt{\frac{1}{2}\left[T \pm \sqrt{T^2 - 4D}\right]}. \qquad (2.28)$$

Of particular interest here is the relationship between the resonant frequencies given by (2.28) and the eigenvalues λ in equation (2.21). This relationship is $\Omega = \sqrt{-\lambda^2}$. This shows that resonance occurs precisely when the forcing frequency matches the natural occurring (centre) oscillations near the equilibrium point.

For the trophic web system discussed by Stone (1990), we now evaluate the resonant frequencies (2.24) explicitly. From the parameter values given by Stone (1990), it is possible to estimate the dimensionless constants of the present investigation to have values $\alpha = 0.4, \beta_0 = 1.2, \gamma = 1.2, \delta = 0.4$ and $\eta = 0.2$. It follows from equation (2.15) that $T = 2.0320$ and $D = 0.5107$. These parameter values will be assumed throughout this chapter. Equation (2.28) therefore shows that there are *two* frequencies Ω=0.5421 and Ω=1.3184 at which primary resonance can occur. In dimensional variables, these are equivalent to periods of about 15 hours and 7 hours respectively, so that these two primary resonances are occurring roughly at diurnal forcing frequencies.

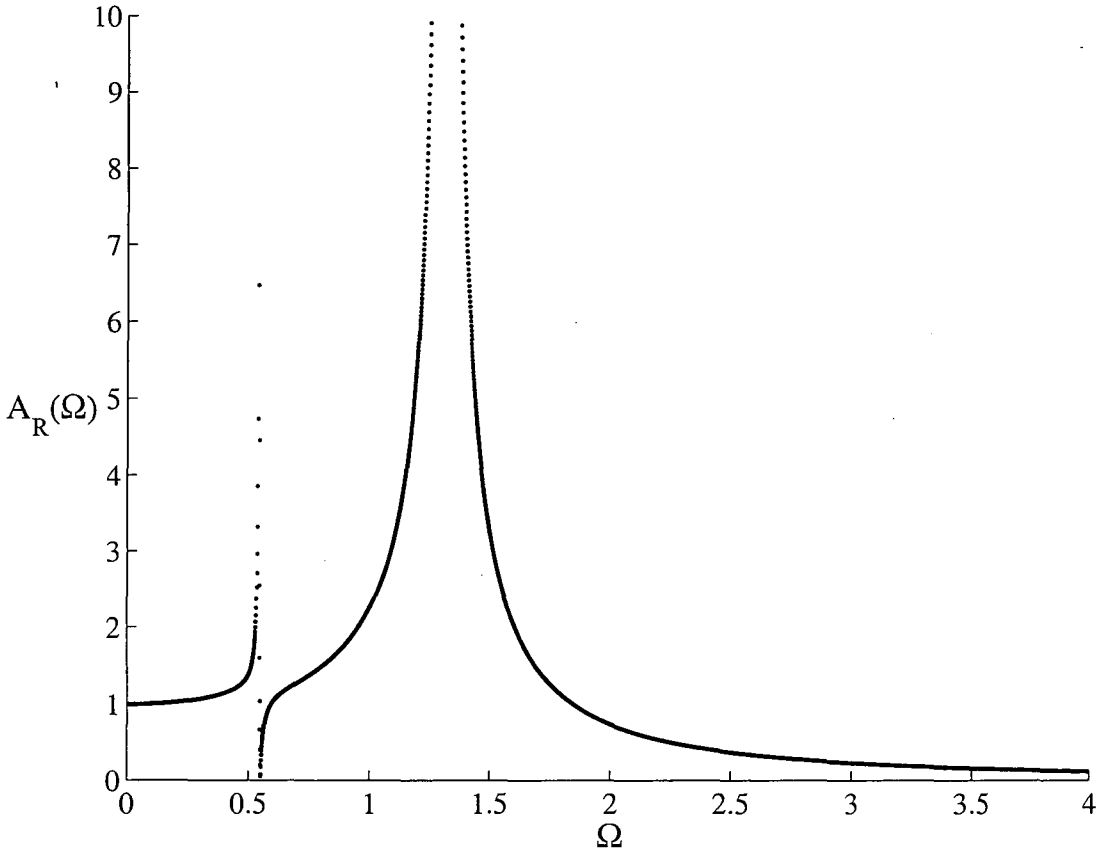

Fig 2.2 The resonance curve showing amplitude against frequency for the linearised solution R_1

Figure 2.2 depicts the change in amplitude |L/M| of the solution $R_1(t)$ of the linear system (2.23) as forcing frequency Ω varies. The diagram shows the two points of primary resonance as Ω=0.5421 and Ω=1.3184, where the amplitude of the linearized solution becomes infinite. Of course, linearization itself is only valid for small amplitudes, and so the linearized solution breaks down near resonance, and non-linear effects dominate. The amplitude in Figure 2.2 falls to zero at the forcing frequency $\Omega = \sqrt{\delta Y} = 0.5514$, where L=0 in equation (2.26).

2.4. Numerical results

This section presents the results of numerical solutions to the fully non-linear system of equations (2.3) with the seasonal forcing term (2.9). The differential equations were integrated in time using the package *MATLAB*.

Figures 2.3-2.5 show a sequence of results of the amplitude of the solution R(t) against the forcing frequency Ω, for three different forcing amplitudes β_1. The period of oscillation in the case of seasonal forcing is $\tau = 2\pi / \Omega$.

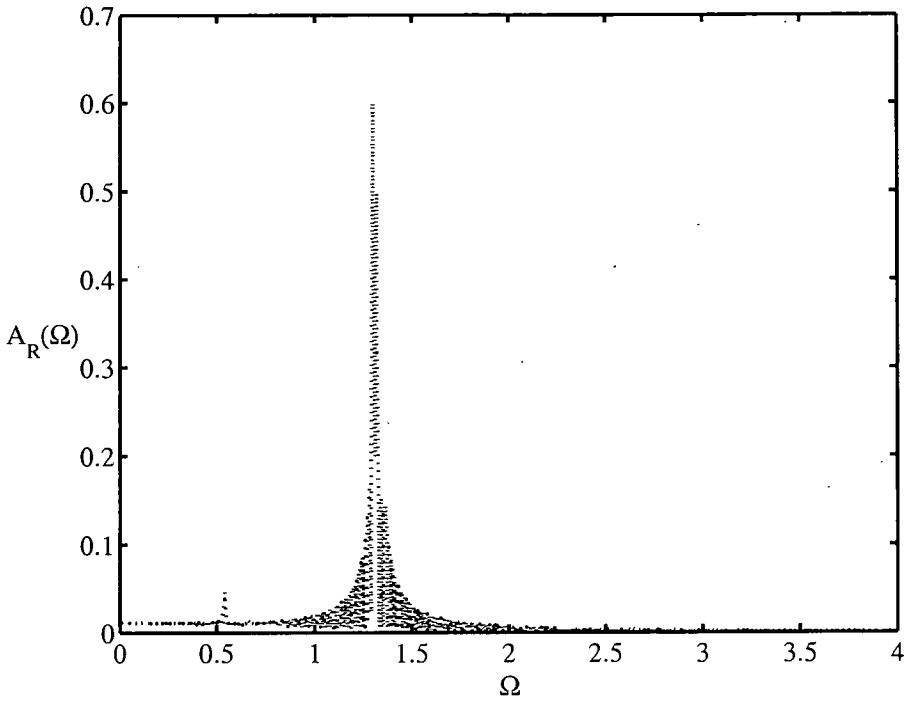

Fig 2.3. The amplitude of the non linear solution R(t) against the forcing frequency Ω for small forcing amplitude $\beta_1 = 0.005$.

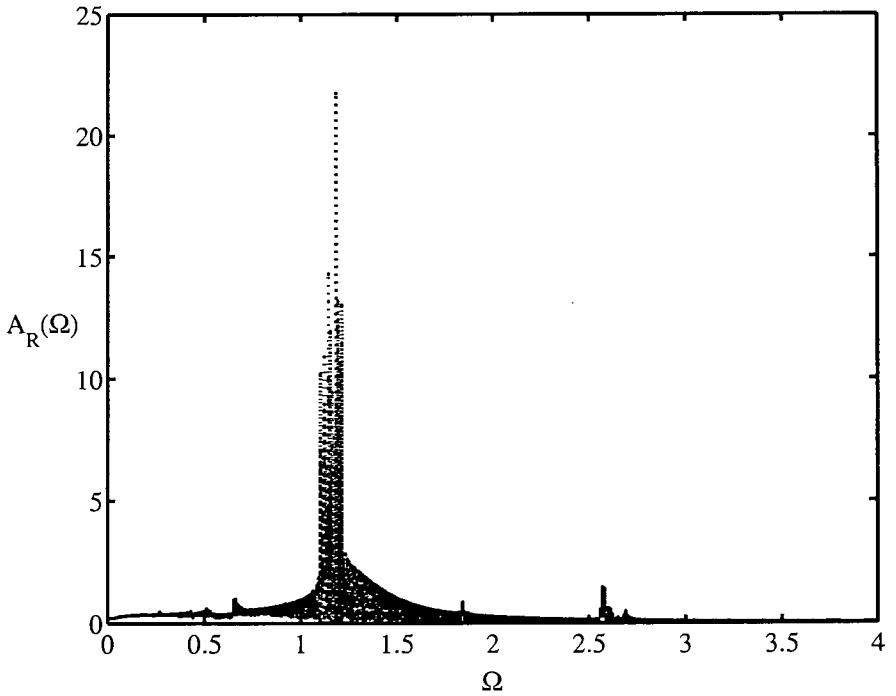

Fig 2.4. Amplitude of R(t) against forcing frequency Ω for moderate forcing amplitude $\beta_1 = 0.2$.

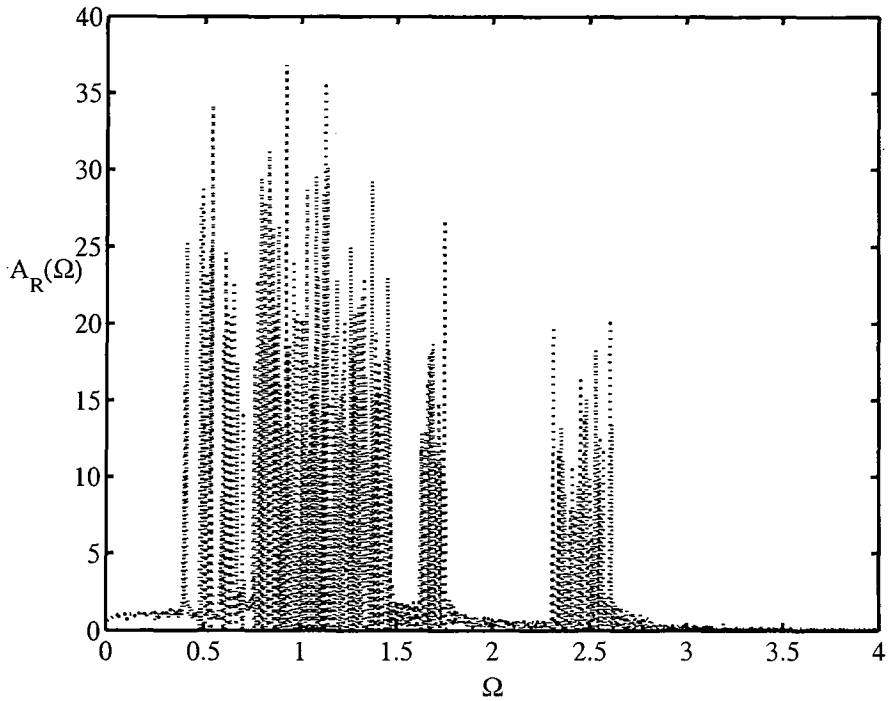

Fig 2.5. Amplitude of the non linear solution R(t) against the forcing frequency Ω for large forcing amplitude β_1=0.6

The results in figures 2.3 - 2.5 were generated by the following method. A differential equation integration routine from the package MATLAB was used to find the solution to the system of equations (2.3), subject to the seasonal forcing term (2.9). The initial point was taken to be (γ, δ/α, (1-$\delta\gamma$)/α, X) and the dimensionless constants α, and so on, were given the values described previously. The numerical solution was integrated forward in time for a large number of forcing periods, typically of the order of 800τ, until transients had died away. The solution R(t) was then recorded for a further 15 forcing periods, and the maximum amplitude for each of these successive periods was plotted as a point on the graph. This process was repeated at each forcing frequency Ω. This permits the effects of resonance and non-linearity to be examined, since a single point on the diagram at a particular frequency corresponds to a period-one solution at that frequency. Two points represents a period double solution, and so on. A continuum of points at a fixed frequency either represents quasi-periodicity or chaos. Figures 2.3 – 2.5 effectively give Poincare cross-sections at each frequency (see Guckenheimer and Holmes, page 22), and so can be regarded as bifurcation plots.

In Fig 2.3 a small forcing amplitude β_1=0.005 was used. Two primary resonance peaks were observed and are visible in the diagram, at frequencies very close to the linearized resonances Ω=0.5421 and Ω=1.3184. For this small forcing amplitude, the non-linear results in Figure 2.3 closely resemble the linearized solution Figure 2.2, as is expected. This confirms the reliability of the current approach.

The forcing amplitude has been increased to the moderate value β_1 = 0.2 to produce the results in Figure 2.4. It is evident that the agreement with the linearized solution is beginning to break down at this forcing amplitude. There is no longer a uniform rise to a

peak at resonance, and instead the peak has broadened significantly. An additional sub-harmonic resonance peak is also visible at a frequency of about $\Omega \approx 2.5$ and is evidence of the increasing role of non-linearity in this solution.

Figure 2.5 shows further increases in the effects of non-linearity. This graph was obtained with large forcing amplitude, β_1=0.6. The primary resonance peak has now been replaced with a broad band of large amplitude forced responses, apparently containing primary and sub-harmonic resonances along with chaotic responses. A secondary large amplitude peak is visible about $\Omega \approx 2.5$.

In the next sequence of three diagrams, the forcing amplitude Ω is held constant, and the linearized and non-linear solutions for R(t) are compared for different values of forcing amplitude. The results are presented in Figures 2.6-2.8

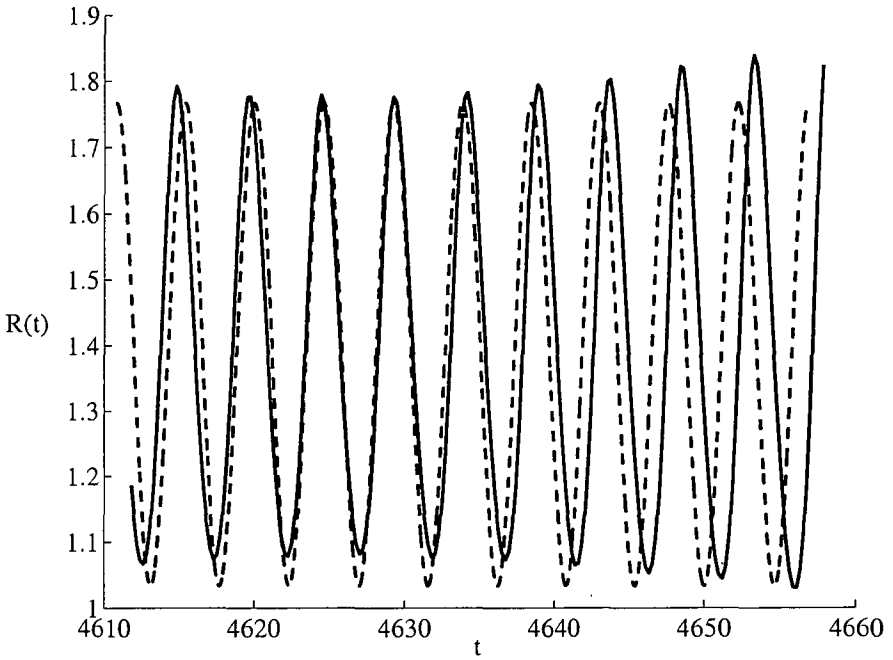

Fig 2.6. Graph of the linear (dashed line) compared with the non-linear solution $R(t)$ with β_1=0.005 and $\Omega = 1.362$

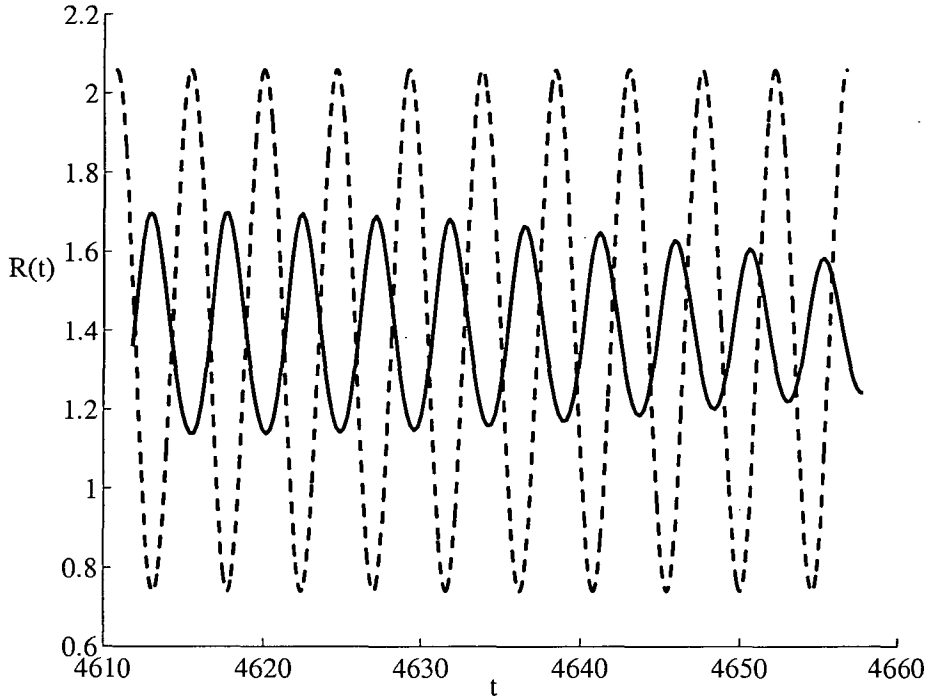

Fig 2.7. Graph of the linear (dashed line) compared with the non-linear solution for $R(t)$ with β_1=0.009 and $\Omega = 1.362$

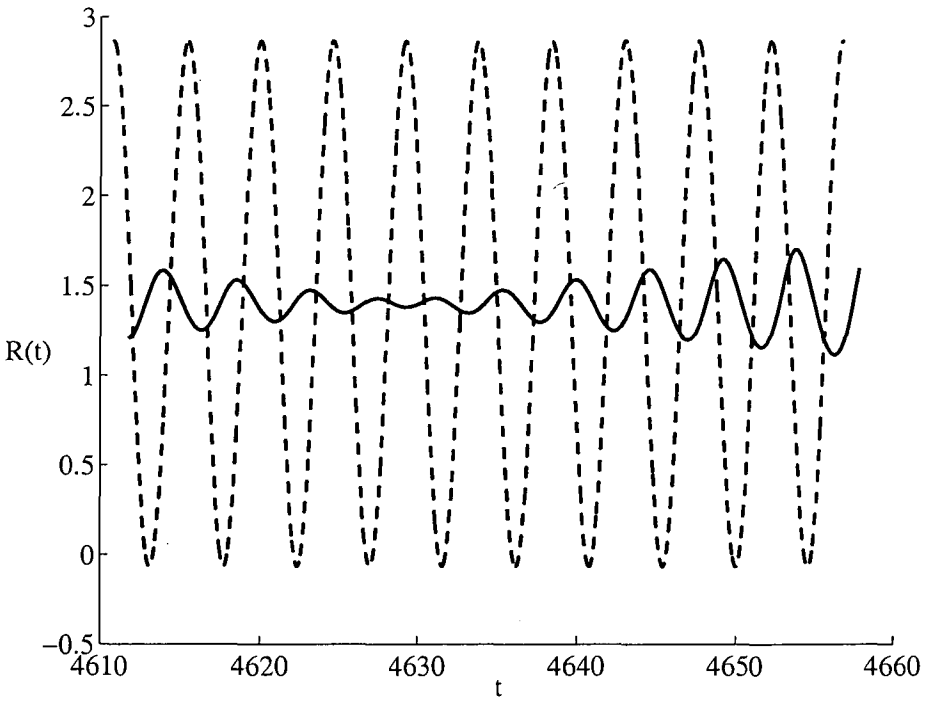

Fig 2.8. Graph of the linear (dashed line) compared with the non-linear solution for $R(t)$ with β_1=0.02 and $\Omega = 1.362$

The linearized solution in Figures 2.6-2.8 has been calculated from the result for *R(t)* given in the equation (2.24), and is sketched with dashed lines in these diagrams. The non-linear solutions were computed using MATLAB to integrate (2.3) forward in time

for 100 periods (100τ), to remove transients due to initial conditions, and then a further 10 periods were computed an presented as solid lines in these graphs. (The same initial conditions were assumed as for the bifurcation diagrams in Figures 2.3-2.5). The forcing frequency $\Omega = 1.362$ has been chosen to be close to the upper primary resonance in the linearized solution.

The results in Figure 2.6 show that the non-linear solution is in reasonably close agreement with the non-linear profile shown, as is broadly to be expected for this small forcing amplitude $\beta_1 = 0.005$. This confirms the reliability of the integration routine. Nevertheless, even at this small forcing amplitude, there is evidence of some non-linear effects. In particular the amplitude of the non-linear solution is not quite constant, suggesting the influence of a high period perturbation, and the period itself is slightly different from that of the purely linearized result.

These effects are more strongly evident in Figure 2.7. The amplitude of the non-linear solution decreases for the ten forcing periods shown in the diagram, but increases again at a later times, giving clear evidence for the existence of a high period orbit. This appears to be associated with quasi-periodic behaviour, as the solution is dominated by several different frequency components that are not rational multiples of one another. This is discussed again later.

The final solution shown in Figure 2.8 gives further evidence of the high period behaviour of the non-linear signal. It is interesting to observe that, for this case, the non-linear solution has very much smaller amplitude than its linearized counterpart. Of course, the linearized solution in Figure 2.8 cannot be expected to retain any validity for this largest forcing amplitude $\beta_1 = 0.2$, in particular since the solution in equation (2.18) predicts that the response amplitude simply increases linearly with forcing amplitude β_1. This would eventually generate negative values for the solution *R(t)* itself, and in fact the result in Figure 2.8 is the largest value of forcing amplitude β_1 for which the linearized solution remains positive for all time.

In Figures 2.9 and 2.10, the non-linear solution is examined further, for forcing amplitudes β_1 larger than those shown in Figures 2.6-2.8. In these next two diagrams, comparison with the linearized solution is no longer possible, as discussed above.

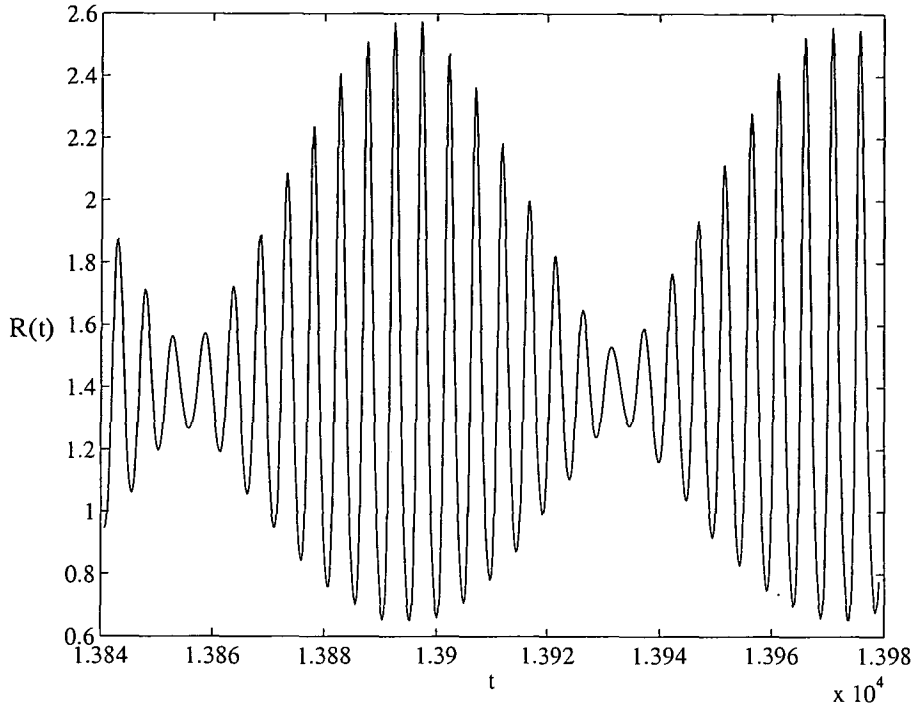

Fig 2.9. Graph of the non-linear solution $R(t)$ against time for β_1=0.05 and $\Omega = 1.362$

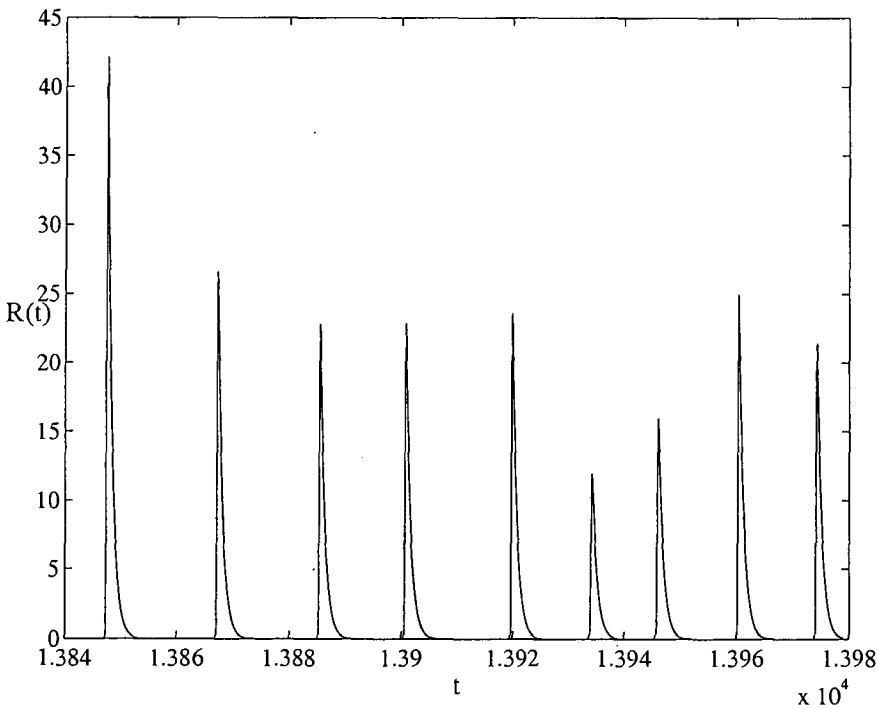

Fig 2.10. Graph of the non-linear solution $R(t)$ against time for β_1=0.2 and $\Omega = 1.362$

The forcing amplitude in Figure 2.9 has been increased to $\beta_1 = 0.05$ and 30 periods (30τ) have now been shown, to give a clear indication of the behaviour of the solution *R(t)*. It is evident that the response curve has indeed become quasi-periodic, with two dominant frequencies. Careful examination of the signal strongly suggests that the solution is not periodic (this is illustrated in Figure 2.11). Quasi-periodicity is known to

be a possible route to chaos, as shown in the theorem of Ruelle, Takens and Newhouse (see the discussion in Thompson and Stewart 1989, page 196). In a recent examination of high-dimensional Lotka-Volterra systems, Sprott et al (2006) likewise found that such systems exhibited quasi-periodic behaviour en route to chaos.

For the result in Figure 2.10, the forcing amplitude has increased further to $\beta_1 = 0.2$. The solution for R(t) now displays intervals of relaxation periods between large peaks, all of dissimilar amplitudes and occurring apparently at random intervals. This stochastic behaviour of the solution (in a deterministic system), coupled with its extreme sensitivity to initial conditions, suggests strongly that chaotic motion has been generated for this forcing amplitude at this frequency.

Further support for the contention that Figures 2.9 and 2.10 are exhibiting quasi-periodic and chaotic behaviours, respectively, can be obtained by considering the solution orbits in the phase space. As the system (2.7) is actually four dimensional, it is not possible to display the full space, but meaningful results can nevertheless be obtained by considering a two-dimensional projection onto the plane. This is done in Figures 2.11 and 2.12 for the two solutions displayed in Figures 2.9 and 2.10, using orbits in a plane consisting of the two variables *R(t)* and *B(t)*. Physically, these represent the populations of the protozoa and the bacteria, and 30 periods are shown.

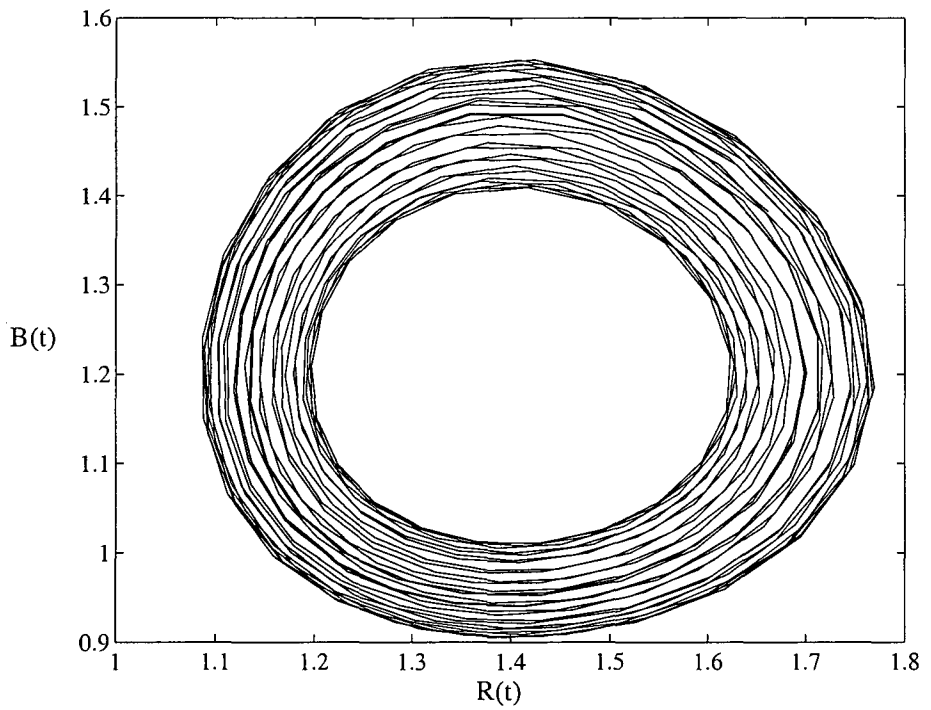

Fig 2.11. Graph of the non-linear solutions $B(t)$ against $R(t)$ for forcing amplitude β_1=0.05 and $\Omega = 1.362$

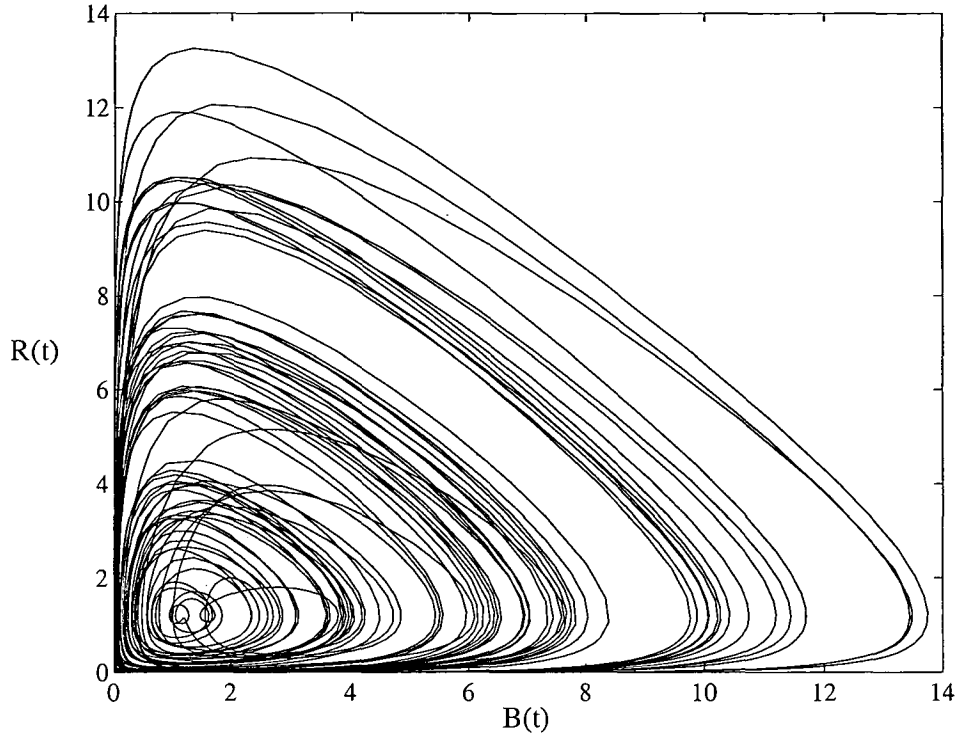

Fig 2.12. Graph of the non-linear solutions $B(t)$ against $R(t)$ for forcing amplitude β_1=0.2 and $\Omega = 1.362$

Figure 2.11 shows a region in the (R, B) plane in which the solution trajectories evidently fill a ring-shaped portion of the plane. This is strongly suggestive of quasi-periodicity, and corresponds to a projection of a high dimensional torus onto the (R, B) plane. Further evidence for this conjecture has been obtained by perturbing these orbits and observing that the solution returns to them, so that they are genuine attractors. The results in Figure 2.12 for the larger forcing amplitude $\beta = 0.2$, however, are more strongly suggestive of chaos. There is clearly no longer a torus structure, but instead the solution trajectories appear to move randomly within some bounded region in the space.

Finally in this results section we look at one example in the non-forced case, shown below in Figure 2.13.

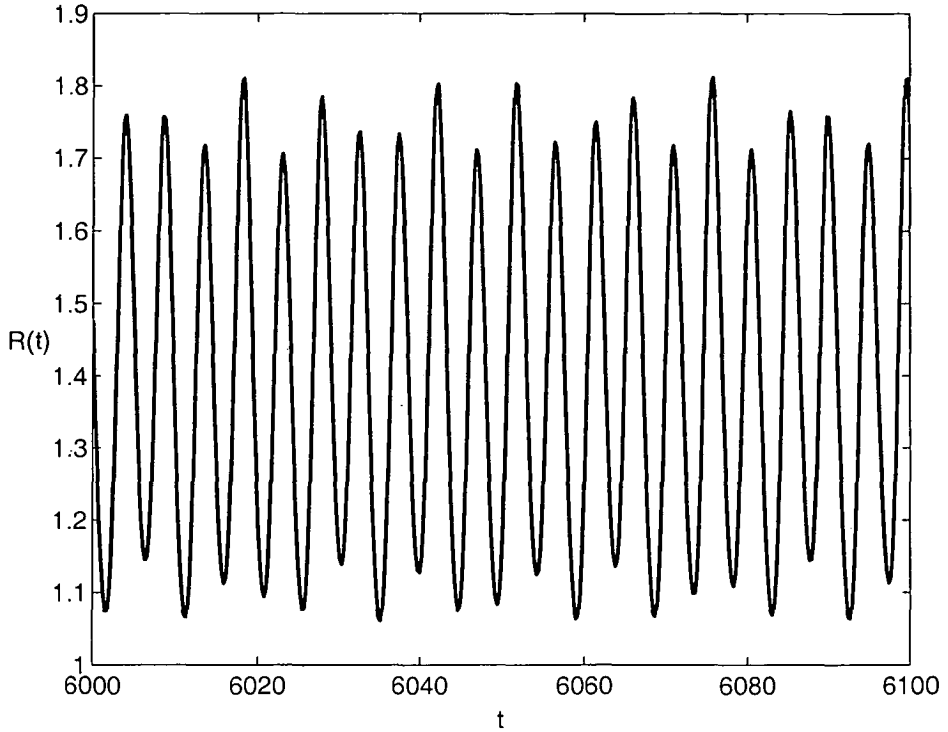

Fig 2.13. Graph of the non-linear solutions $R(t)$ against t for non-forced case. The solution was found at a small perturbation from the fifth equilibrium point in (2.11)

In Figure 2.13 we show a solution to the non-forced case at a small perturbation from the fully populated steady-state in (2.11). As we can see from this picture, non-linear centre behaviour seems to be occurring (with a combination of frequencies). This was predicted by the linear approximation (2.16) of the system near this point; however, as previously stated, this does not necessarily mean that centre behaviour must occur in the non-linear case, since the Hartmann theorem no longer holds. Nevertheless, Figure (2.13) does indeed indicate that centre behaviour appears to be happening in the non-linear case also. To determine whether the solution shown in Fig 2.13 is periodic or quasi-periodic, it was drawn in the R-B phase plane. This gave a closed loop and so we conclude that within numerical error, the solution is indeed likely to be periodic.

2.5. Discussion

This section presented a detailed mathematical investigation of the structure of the solutions to two-level trophic food web model proposed by Stone (1990). Although we have simplified the model by assuming that nutrient is in vast over supply, the system is nevertheless non-linear, due to the interactions between the competing species. As a

result, the unforced system predicts five steady-states. Of these equilibria, only one gives long term survival of all four species. There is another equilibrium point at the origin of the phase space, corresponding to total extinction. Four of the equilibrium points are unstable, and the one for which all populations survive is a centre.

Seasonal or daily forcing has also been studied for this model, based on a sinusoidal variation in the breeding rate for bacteria. At small forcing amplitude there was reasonable agreement between the linear and non-linear solutions, as expected. The linearized solution provides considerable insight into a number of aspects of the global behaviour, including the identification of two forcing frequencies at which primary resonance occurs. Agreement between the numerical results and the linearized solution for small amplitudes therefore serves as a valuable check on the reliability of the non-linear solution.

For the parameter values used here, taken from the paper by Stone (1990), primary resonance has been found to occur at $\Omega \approx 1$, which corresponds to a forcing frequency ω of the order of 1 day^{-1}. These results are therefore appropriate to daily forcing, consistent with the work of Edwards *et al* (1999).

As the forcing amplitude is increased, the agreement with linearized theory breaks down, as is to be expected. The non-linear results exhibit rich diversity of complex behaviour, including high-period orbits, sub-harmonic resonances, quasi-periodicity and chaos. The results strongly suggest that, as amplitude is increased for a fixed forcing frequency, quasi-periodicity may lead to chaos via a Ruelle-Takens-Newhouse bifurcation.

It is appropriate to ask whether, in a real biological system, the forcing amplitudes could ever become sufficiently large for the more exotic non-linear effects predicted here to be observed in practice. From Stones' paper (1990), the unforced breeding rate, in dimensionless variables, has the value $\beta_0 = 1.2$, and the relative perturbation to this due to forcing is simply β_1 / β_0, from equation (2.5). The quasi-periodic solutions illustrated in Figures 2.9 and 2.11 were obtained with forcing amplitude $\beta_1 = 0.05$, and this represents only a 4% variation to the unforced reproduction rate. Event the chaotic results of Figures 10 and 12, with $\beta_1 = 0.2$, represent only a 17% variation, and we therefore conclude that highly non-linear behaviour, including chaos, is a likely feature of such trophic web systems.

It has been assumed here that the nutrients N are in unlimited supply. When this is no longer true, even more rich dynamic behaviour may be possible. In particular, the four-dimensional system studied here is essentially degenerate, in the sense that the unforced equations give rise to equilibrium points that are centres. When variation in nutrient concentrations are also allowed, it is possible that these points may allow Hopf bifurcations to be present., so raising the additional complexity of limit cycles and their forced equivalents in the seasonally varying case. An investigation of the effects of varying nutrient concentration is the subject of the next chapter.

CHAPTER 3

Nutrient Uptake Model

In the last chapter we examined the model proposed by Stone (1990), in the case where the nutrients N were in unlimited supply. We now consider the situation in which nutrient supply is limited. The original question posed by Stone (1990) aimed at investigating the behaviour of the system when the nutrient supply is low. We mentioned in the first chapter how Stone (1990) aimed to show that the paradoxical behaviour of the Phytoplankton (stimulating the growth of its competitor) was due to indirect effects. This was assumed to be equivalent to feedback within the system. Feedback, in a biological model, refers to the situation where the product of one interaction effects other interactions (see Murray (1989) for further discussion). On the basis of this assumption we excluded the nutrient term as, although it added to the complexity of the system, it does not qualitatively add to the notion of feedback control mechanics. However, adding a nutrient term and making the interaction functions dependant on nutrient concentrations does change the dynamics of the problem (by adding an extra feedback mechanism). In order to investigate the model more fully we now consider including a nutrients term in the model.

There has been much work done on the effect of interaction functions in dynamical systems. It has been shown by Gross et al (2004) that Holling II, or Michaelis-Menten, type interaction functions can either destabilize or stabilize steady-states, dependent on the form of the interaction function used. A change in stability is achieved by enriching one of the populations. This was found to be an underlying idea in the "paradox of enrichment" (Edwards et al 1999). We will be using a Michaelis-Menten term for the growth rates, which are now nutrient dependant. This will be discussed in more detail further on, and a more comprehensive discussion of this idea is given by Murray (1989).

We will introduce a fifth equation into the set of governing equations derived in the last chapter. This will account for the rate of change of nutrient concentrations in the system and will be linked to the species populations. The growth rates of the phytoplankton and bacteria will also now depend on the nutrient supply, as mentioned, and therefore their reproduction rates will be represented by a nutrient dependent term.

The equilibrium points for the nutrient-independent model had at least two purely imaginary eigenvalues. In the forced system, quasi–periodicity was suggested to be present, on the basis of the numerical results. We did not, however, find any Hopf bifurcations in the unforced case. In this chapter we will investigate the possibility that the introduction of variable nutrient concentration in the unforced system will generate instability in the steady-state, causing self-sustained oscillations to occur in the solutions, which will result in limit cycles being formed (possibly as the result of a Hopf bifurcation).

In this chapter we therefore expand upon the work done in the previous chapter on Stone's (1990) model. Once again, ideas from the theory of dynamical systems (see Murray 1989, Edelstein-Keshet 1988 for more discussion) are used here to investigate the stability of steady-state populations and the possibility of self sustained oscillations. The model is non-linear and with the introduction of a nutrient term and nutrient dependent interaction functions we find a Hopf bifurcation present. This leads to self sustained oscillations. We examine the stability of the limit cycles using Floquet theory.

The model is presented in Section 3.1 and for convenience scaled (non-dimensional) populations and rates are introduced as in the previous chapter. In Section 3.2 we provide an analysis of the model including finding a Hopf bifurcation. For an arbitrary value of the Nutrient concentration, we find a solution branch of limit cycles and test the stability of the branch. We end this chapter with a discussion of the results.

3.1. The Mathematical Model

The trophic web considered now is that illustrated the previous chapter in Fig 2.1, from Stones' original paper, where once again, the direction of the interaction is given by the arrows.

From our initial assumption in the previous chapter, that the nutrients were in unlimited supply, the system of equations described by Fig 2.1 is given below. This is the situation already described in chapter 2.

$$\begin{aligned} dB/dt &= r_b B - r_r RB + r_i PB \\ dP/dt &= r_p P - r_z PZ - r_i BP \\ dZ/dt &= r_z PZ - d_z Z \\ dR/dt &= r_r RB - d_r R. \end{aligned} \tag{3.1}$$

We now assume that the reproductive rates of the Bacteria and Phytoplankton, r_b and r_p respectively, depend on the nutrient concentration N. We are using a Michaelis-Menten uptake term for nutrients by bacteria, so that the reproductive rate for bacteria is governed by the equation

$$r_b(N) = \frac{k_b N}{a_b + b_b N} \quad . \tag{3.2}$$

This term reflects the saturation effects seen in the nutrient uptake process, whereby an infinite supply of nutrients will not result in the unlimited growth of bacteria in the presence of predators. The terms a_b, b_b, k_b, are constants that determine the rate of

uptake of the nutrients. In their paper Gross et al (2004) showed a situation where, for Holling II type interaction functions like (3.2), enrichment (increase in a population) destabilized the steady-state solutions of a general food chain similar to the one being considered.

In the previous chapter we assumed that N did not change and therefore had some fixed value N_0 say. Using (3.2) we get the initial value for the reproductive rate as used in the last chapter as being,

$$r_{b0} = \frac{k_b N_0}{a_b + b_b N_0} \tag{3.3}$$

We can incorporate (3.3) into the nutrient dependent reproductive rates by dividing through by this term, as seen below.

$$\frac{r_b(N)}{r_{b0}} = \frac{k_b N/(a_b + b_b N)}{k_b N_0/(a_b + b_b N_0)} \tag{3.4}$$

We can now express the nutrient dependent reproductive rates $r_b(N)$, $r_p(N)$ in the equivalent form

$$r_b(N) = \frac{r_{b0}(N/N_0)}{1 + c_b(N/N_0 - 1)},\ r_p(N) = \frac{r_{p0}(N/N_0)}{1 + c_p(N/N_0 - 1)} \tag{3.5}$$

In this sense we have said that if $N = N_0$, and remains fixed we would have the same system as represented by (3.1). Equations (3.5) therefore generalize the system, discussed in chapter 2, to the case where nutrient concentration may now vary.

In chapter 2 we showed the reproductive rates with a forcing term. For completeness, we show these again here, although the effects of forcing in this more complicated system will not be considered. With forcing these rates become

$$r_b(N) = \frac{[r_{b0} + r_{b1}\cos\Omega t](N/N_0)}{1 + c_b(N/N_0 - 1)},\ r_p(N) = \frac{[r_{p0} + r_{p1}\cos\Omega t](N/N_0)}{1 + c_p(N/N_0 - 1)}$$

In equation (3.5) N is the concentration of nutrient. We assume now that the total mass of the system, including all the organisms, is constant, in which case we have

$$N + m_B\dot{B} + m_P P + m_Z Z + m_R R = N_0\ . \tag{3.6}$$

Here, m_i is the mass of nutrient in each individual in B,P,R and Z. Since B, P, Z and R represent the population per volume, a term such as $m_B B$ represents the mass of nutrient per organism multiplied by the number per volume, which gives us a

concentration (since number is dimensionless). The rate of change of mass of nutrient in the whole system is equal to zero, and thus equation (3.6) leads at once to

$$\frac{dN}{dt} + m_B \frac{dB}{dt} + m_P \frac{dP}{dT} + m_Z \frac{dZ}{dt} + m_R \frac{dR}{dt} = 0 . \qquad (3.7)$$

We substitute equations (3.1) into (3.7) to give

$$\frac{dN}{dt} + m_B (r_b B - r_r RB + r_i BP) + m_P (r_p P - r_z PZ - r_i BP) + m_Z (r_z PZ - d_Z Z) + m_R (r_r RB - d_r R) = 0 . \qquad (3.8)$$

For simplicity, we now make the approximation that $m_B = m_P = m_Z = m_R = m$, that is, that all the organisms contain roughly the same mass of nutrients. As a result, equation (3.8) assumes the form

$$\frac{1}{m}\frac{dN}{dt} + (r_b B + r_p P) - (d_r R + d_z Z) = 0 . \qquad (3.9)$$

The model, without forcing, with nutrients included is fully described by the following set of equations;

$$dB/dt = r_b B - r_r RB + r_i PB$$

$$dP/dt = r_p P - r_z PZ - r_i BP$$

$$dZ/dt = r_z PZ - d_z Z \qquad (3.10)$$

$$dR/dt = r_r RB - d_r R$$

$$\frac{1}{m}\frac{dN}{dt} = -r_b B - r_p P + d_r R + d_z Z$$

in which the rates are now given by equations (3.5).

Using the same method shown in Chapter 2, we re-cast (3.10) in terms of dimensionless variables. In this case, the four populations (B, P, Z, R) are scaled with respect to the quantity r_{p0} / r_r, which is a naturally occurring measure of population as stated in the last chapter. The nutrient concentration N, is scaled with respect to the quantity N_0, which is arbitrary and so this choice has no implications for the dynamics of the system. Once again, time t is made dimensionless using the quantity $1/r_{p0}$, which is a time scale linked roughly to the life-cycle of the phytoplankton, as already stated in Chapter 2. In these non-dimensional variables, equations (3.10) become

$$\frac{dB}{dt} = \beta\left[\frac{N}{1+c_b(N-1)}\right]B - RB + \eta BP$$

$$\frac{dP}{dt} = \left[\frac{N}{1+c_p(N-1)}\right]P - \alpha PZ - \eta BP$$

$$\frac{dZ}{dt} = \alpha PZ - \delta Z$$

$$\frac{dR}{dt} = RB - \gamma R$$

$$\frac{dN}{dt} = \mu\left[-\beta\left[\frac{N}{1+c_b(N-1)}\right]B - \left[\frac{N}{1+c_p(N-1)}\right]P + \gamma R + \delta Z\right] \qquad (3.11)$$

The constant $\mu = \frac{mP_s}{N_0}$ is such that $0 < \mu < 1$, a result that can be deduced from (3.6). The parameters $\alpha, \beta, \gamma, \delta, \eta$ are the same as in Chapter 2.

3.2 Analysis of the Model

3.2.1 Steady-state populations

We now look for the steady state solutions (B, P, Z, R, N) which satisfy

$$dB/dt = dP/dt = dZ/dt = dR/dt = dN/dt = 0.$$

We choose $N = N_0$, where now N_0 represents some arbitrary dimensionless initial concentration of nutrient. This yields the four equilibrium points

$$(0,0,0,0,N_0)\ ,\ (\gamma,0,0,\beta K,N_0),\ (0,\delta/\alpha,K_1/\alpha,0,N_0),$$
$$(\gamma,\delta/\alpha,K_1-\eta\gamma/\alpha,\beta K+\eta\delta/\alpha,N_0)\quad , \qquad (3.12)$$

where $K = \frac{N_0}{1+c_{b0}(N_0-1)}$, $K_1 = \frac{N_0}{1+c_{p0}(N_0-1)}$. (3.13)

In (3.13) c_{b0}, c_{p0} are the nutrient uptake rates for the bacteria and phytoplankton respectively. The first steady state in (3.12) represents the case where only the nutrients remain, and all the species die out. The second and third steady states are where two species, a predator and prey coupling, survive. The fourth steady-state, which is of most interest to our analysis, is where all the species survive. We will now look to ascertain the stability of these states. It should be mentioned that two more steady-states were

found; however they contained negative values for some of the populations and as such were unrealisable in an actual situation.

3.2.2 Stability of the Steady-states

Following the same method used in chapter 2 the linear approximations, shown in (3.14), to the solutions close to steady-states are used.

$$\begin{aligned} B(t) &= B_{eq} + \varepsilon B_1 + O(\varepsilon^2) \\ P(t) &= P_{eq} + \varepsilon P_1 + O(\varepsilon^2) \\ Z(t) &= Z_{eq} + \varepsilon Z_1 + O(\varepsilon^2) \\ R(t) &= R_{eq} + \varepsilon R_1 + O(\varepsilon^2) \\ N(t) &= N_{eq} + \varepsilon N_1 + O(\varepsilon^2) \end{aligned} \qquad (3.14)$$

As already stated in the previous chapter, the constant ε represents how close the system is to one of its steady states. We determine the linearized system near an equilibrium point by substituting (3.14) into the governing equations (3.11) and retaining terms at the first order in ε.

When equations (3.14) are substituted into the first equation in the system (3.11), the term dB/dt is represented as

$$\begin{aligned} \frac{d}{dt}\left[B_{eq} + \varepsilon B_1\right] = \beta &\left(\frac{N_{eq}B_{eq} + \varepsilon\left[N_1 B_{eq} + B_1 N_{eq}\right]}{1 + c_{b0}\left[N_{eq} + \varepsilon N_1 - 1\right]} \right) \\ &- \left(R_{eq}B_{eq} + \varepsilon\left[R_{eq}B_1 + B_{eq}R_1\right]\right) + \eta\left(B_{eq}P_{eq} + \varepsilon\left[B_1 P_{eq} + P_{eq}B_1\right]\right). \end{aligned} \qquad (3.15)$$

In order to proceed, it is necessary to make use of the geometric series

$$\frac{1}{1+Z} = 1 - Z + Z^2 - Z^3 \ldots\ldots \qquad \text{for } |Z| < 1 \,. \qquad (3.16)$$

The first term on the right-hand side of equation (3.15) is written as

$$\beta\left[N_{eq}B_{eq} + \varepsilon\left(N_1 B_{eq} + B_1 N_{eq}\right)\right] \frac{1}{\left(1 + c_{b0}\left(N_{eq} - 1\right)\right)} \left[\frac{1}{1 + \varepsilon\left(\frac{c_{b0}N_1}{1 + c_{b0}(N_{eq} - 1)} \right)} \right]$$

(3.17)

We then make use of (3.16) to re-write (3.17) in the form

$$\frac{\beta}{1+c_{b0}\left(N_{eq}-1\right)}\left[N_{eq}B_{eq}-\varepsilon\left(\frac{c_{b0}N_{eq}B_{eq}N_1}{1+c_{b0}\left(N_{eq}-1\right)}\right)+\varepsilon\left(N_1B_{eq}+B_1N_{eq}\right)+O(\varepsilon^2)\right].$$

(3.18)

Equation (3.18) is now used in equation (3.15), along with the steady-state identity

$$\frac{dB_{eq}}{dt}=\beta\left(\frac{B_{eq}N_{eq}}{1+c_{b0}\left(N_{eq}-1\right)}\right)+R_{eq}B_{eq}+\eta B_{eq}P_{eq}=0\ .$$

Retaining terms to the first order in ε then gives the linearized form of the first equation in the system (3.11). When the similar procedure is applied to each such equation, we obtain the linearized equivalent of the entire system of equations (3.11) in the form,

$$\frac{dB_1}{dt}=\beta\left(\frac{-c_{b0}N_{eq}B_{eq}N_1}{\left(1+c_{b0}\left(N_{eq}-1\right)\right)^2}+\frac{N_1B_{eq}+B_1N_{eq}}{1+c_{b0}\left(N_{eq}-1\right)}\right)-R_1B_{eq}-B_1R_{eq}+\eta\left(B_1P_{eq}+P_1B_{eq}\right)$$

$$\frac{dP_1}{dt}=\left(\frac{-c_{p0}N_{eq}P_{eq}N_1}{\left(1+c_{p0}\left(N_{eq}-1\right)\right)^2}+\frac{N_1P_{eq}+P_1N_{eq}}{1+c_{p0}\left(N_{eq}-1\right)}\right)-\alpha\left(P_1Z_{eq}+Z_1P_{eq}\right)-\eta\left(B_1P_{eq}+P_1B_{eq}\right)$$

$$\frac{dZ_1}{dt}=\alpha\left(P_1Z_{eq}+P_{eq}Z_1\right)-\delta Z_1$$

$$\frac{dR_1}{dt}=\left(R_1B_{eq}+R_{eq}B_1\right)-\gamma R_1 \qquad (3.19)$$

$$\frac{dN_1}{dt}=\mu(-\beta\left(\frac{-c_{b0}N_{eq}B_{eq}N_1}{\left(1+c_{b0}\left(N_{eq}-1\right)\right)^2}+\frac{N_1B_{eq}+B_1N_{eq}}{1+c_{b0}\left(N_{eq}-1\right)}\right)$$

$$-\left(\frac{-c_{p0}N_{eq}P_{eq}N_1}{\left(1+c_{p0}\left(N_{eq}-1\right)\right)^2}+\frac{N_1P_{eq}+P_1N_{eq}}{1+c_{p0}\left(N_{eq}-1\right)}\right)+\gamma R_1+\delta Z_1\ )$$

Gathering the terms with respect to each population, we can produce the following linear matrix system which we use to find the characteristic equation of this system at each equilibrium point.

$$d/dt\begin{bmatrix} B_1 \\ P_1 \\ Z_1 \\ R_1 \\ N_1 \end{bmatrix} = \begin{bmatrix} J_{11} & \eta B_{eq} & 0 & -B_{eq} & J_{15} \\ -\eta P_{eq} & J_{22} & -\alpha P_{eq} & 0 & J_{25} \\ 0 & \alpha Z_{eq} & \alpha P_{eq} - \delta & 0 & 0 \\ R_{eq} & 0 & 0 & B_{eq} - \gamma & 0 \\ -\mu\beta K & -\mu K_1 & \mu\delta & \mu\gamma & J_{55} \end{bmatrix} \begin{bmatrix} B_1 \\ P_1 \\ Z_1 \\ R_1 \\ N_1 \end{bmatrix} \qquad (3.20)$$

Here,

$$\begin{aligned} J_{11} &= \beta K - R_{eq} + \eta P_{eq} \\ J_{15} &= \beta\left(\frac{-c_{b0}N_{eq}B_{eq}}{\left(1+c_{b0}\left(N_{eq}-1\right)\right)^2} + \frac{B_{eq}}{1+c_{b0}\left(N_{eq}-1\right)}\right) \\ J_{22} &= K_1 - \alpha Z_{eq} - \eta B_{eq} \\ J_{25} &= \frac{-c_{p0}N_{eq}P_{eq}}{\left(1+c_{p0}\left(N_{eq}-1\right)\right)^2} + \frac{P_{eq}}{1+c_{p0}\left(N_{eq}-1\right)} \\ J_{55} &= -\mu\left(J_{15}+J_{25}\right) \end{aligned} \qquad (3.21)$$

are defined for convenience.

We are only interested here in the steady-state where all the populations survive. We substitute this equilibrium point $\left(\gamma, \delta/\alpha, K_1 - \eta\gamma/\alpha, \beta K + \eta\delta/\alpha, N_0\right)$, into (3.20) to produce the Jacobian matrix

$$\begin{vmatrix} 0 & \gamma\eta & 0 & -\gamma & E_{15} \\ \frac{-\eta\delta}{\alpha} & 0 & -\delta & 0 & E_{25} \\ 0 & E_{32} & 0 & 0 & 0 \\ E_{41} & 0 & 0 & 0 & 0 \\ -\mu\beta K & -\mu K_1 & \mu\delta & \mu\gamma & E_{55} \end{vmatrix} \qquad (3.22)$$

In this expression (3.22), it has proved convenient to define the intermediate quantities

$$\begin{aligned} E_{15} &= \frac{\beta\gamma\left(1-c_{b0}\right)}{\left(1+c_{b0}\left(N_0-1\right)\right)^2} \\ E_{25} &= \frac{\delta\left(1-c_{p0}\right)}{\alpha\left(1+c_{p0}\left(N_0-1\right)\right)^2} \\ E_{32} &= K_1 - \eta\gamma \\ E_{41} &= \beta K + \eta\delta/\alpha \end{aligned}$$

$$E_{55} = -\mu(E_{15} + E_{25}) \ .$$

The eigenvalues λ for the linearized system (3.20), with coefficient matrix (3.22), are found from the characteristic equation

$$-\lambda^5 + Q_4\lambda^4 + Q_3\lambda^3 + Q_2\lambda^2 + Q_1\lambda = 0 \ , \qquad (3.23)$$

in which it is convenient to define

$$Q_1 = -E_{32}E_{41}\gamma\delta + E_{25}E_{41}\mu\gamma^2\eta - \mu\gamma K_1 E_{25}E_{41} - E_{15}E_{32}\frac{\mu\delta^2\eta}{\alpha} - E_{15}E_{32}\mu\beta\delta K$$

$$Q_2 = E_{41}E_{55}\gamma + E_{15}E_{41}\mu\gamma + E_{32}E_{55}\delta + E_{25}E_{32}\mu\delta + E_{55}\frac{\eta^2\delta\gamma}{\alpha} - E_{25}\mu\beta\eta\gamma K + E_{15}\frac{\mu\delta\eta}{\alpha}K_1$$

$$Q_3 = -E_{41}\gamma - E_{32}\delta - E_{25}\mu K_1 - \frac{\eta^2\delta\gamma}{\alpha} - E_{15}\mu\beta K$$

$$Q_4 = E_{55} \ . \qquad (3.24)$$

In order for there to be a Hopf Bifurcation present we need there to be at least one pair of complex conjugate eigenvalues whose real part vanishes. For this to happen equation (3.23) must be in the form

$$(\lambda + ip)(\lambda - ip)\left(-\lambda^3 + b_2\lambda^2 + b_1\lambda\right) = 0 \qquad (3.25)$$

We now expand (3.25) into the form

$$-\lambda^5 + b_2\lambda^4 + \left(b_1 - p^2\right)\lambda^3 + p^2 b_2\lambda^2 + p^2 b_1\lambda = 0 \qquad (3.26)$$

We perform a comparison between the corresponding coefficients of powers of λ given in (3.23) and (3.26) so that

$$b_2 = Q_4, \quad b_1 - p^2 = Q_3, \quad p^2 b_2 = Q_2, \quad p^2 b_1 = Q_1 \qquad (3.27)$$

We solve these sets of criteria to find p and the coefficients b_0, b_1, b_2 in terms of the quantities in equations (3.24). This enables us to find the following conditions necessary for a Hopf bifurcation to be present in the system (3.11);

(i) $\dfrac{Q_2}{Q_4} > 0$,

(ii) $Q_1 Q_4^{\,2} - Q_3 Q_2 Q_4 - Q_2^{\,2} = 0$,

(iii) $Q_3^{\,2} + 4Q_1 > 0$,

(iv) $Q_1 < 0$. $\qquad (3.28)$

The inequalities (i),(iii) and (iv) are a consequence of the need to ensure that the quantity p^2 in equation (3.27) remains positive, to satisfy the necessary conditions for the Hopf bifurcation. The condition (ii) results from solving eqns (3.27) for the quantities $Q_1,..,Q_4$. We solved the above conditions numerically to find a set of parameter values consistent with a Hopf bifurcation. We found that by varying the values of the parameters β and η from those derived in Stone's original paper (α,γ,δ were kept the same as shown in Chapter 2) we were able to find a set of parameter values for which a Hopf bifurcation is possible in the system. The parameters β and η were kept within the realms of physical probability; they were in fact less than the values determined from the rate constants used in Stone's (1990) paper. The Hopf curve is pictured below (Fig 3.1) and it shows the location in the ($N_0-\beta$) parameter-space of the locations in which conditions (3.28) are satisfied, and therefore gives the parameter values at which non-linear oscillatory limit cycles might be expected to be born.

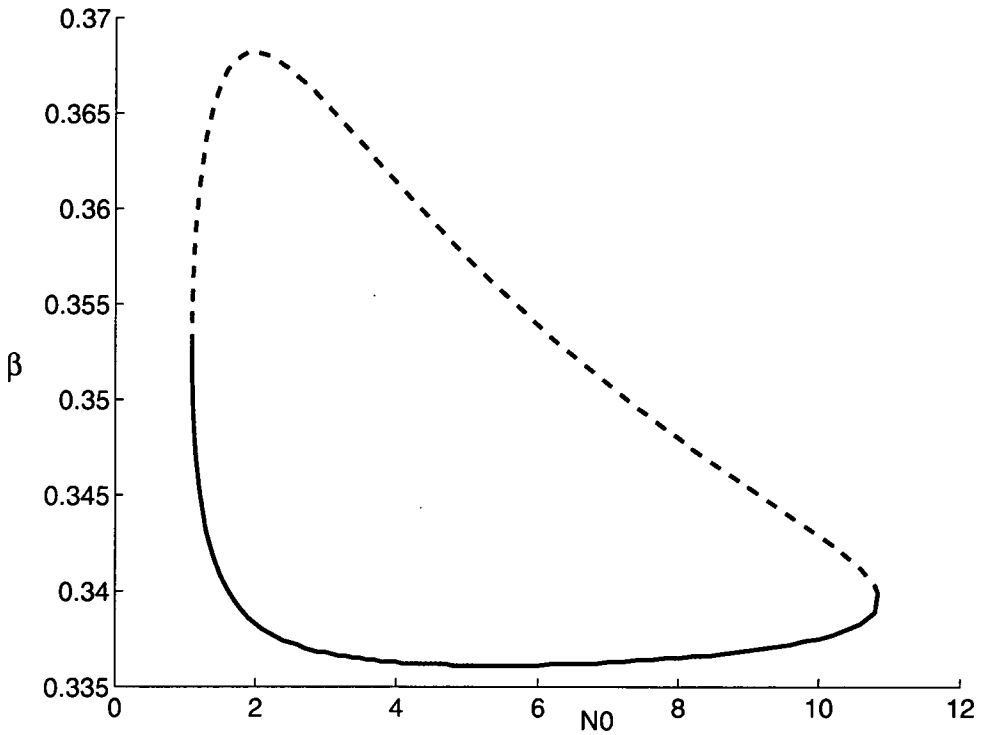

Fig. 3.1 The Hopf curve: The curve shows the location in (N_0,β) space at which oscillatory solutions are born. The smooth line shows the supercritical hopf points and the dashed lines shows the subcritical hopf points. Here $\alpha=0.4,\gamma=1.2,\delta=0.4,\eta=0.01,c_{b0}=0.1,c_{p0}=0.1,\mu=0.1$

Self sustained oscillations born from a Hopf bifurcation occur for values of β on or inside the curve. The Hopf bifurcation first appears at $N_0=1.092$. Each successive value of N_0 has two Hopf points, a supercritical (continuous line) and subcritical (dashed line) Hopf point. The supercritical Hopf points give rise to stable limit cycles (as determined in sec 3.3) and the subcritical point give unstable limit cycles. The

supercritical and subcritical branches converge again at $N_0 = 10.82$, after which the Hopf criteria (3.28) are no longer satisfied for the current parameter values.

Shertzer et al (2002) showed that predator-prey models of systems, where the prey have developed defences to attack, have the best fit with experimentation and that limit cycles are born from the terms modelling the defence mechanism. The existence in this model of an interaction between Bacteria and Phytoplankton acts as a de-facto defence mechanism, at least in the sense that it is responsible for the generation of limit cycles at low nutrients; this has some similarities with a more sophisticated defence model proposed by Shertzer (2002). Our analysis shows that self-sustained oscillations in the unforced system are possible. The oscillations take the form of limit cycles arising out of a Hopf bifurcation (periodic oscillations of species over time in a closed system) which will be investigated further in section 3.3.

3.3 Numerical results

As in chapter 2 we used MATLAB to solve the non-linear system at the parameter values discussed in the previous section. Once we were satisfied that apparently oscillatory solutions were present then, using a shooting method based on Newton's method, we were able to find if the resultant solutions were in fact periodic limit cycles. The method used will now be described briefly here.

The stability of a limit cycle can be determined using Floquet theory. This works by perturbing near the limit cycle. For an n-dimensional system, there are n orthogonal directions in which the perturbation could occur. One of these is along the limit cycles itself, and so is neutrally stable; it therefore gives an eiganvalue equal to 1 in the monodromy matrix. The remaining n-1 eigenvalues determine stability. If the eigenvalues are less than 1 in absolute value then the limit cycle is stable, other wise unstable. For a more in depth discussion see Seydel (1994).

We re-scaled equations (3.11) by introducing a new time variable

$$\tau = t\frac{2\pi}{P_t}$$

where P_t is the period of oscillation, and is as yet unknown. We made a guess for the initial conditions [B(0),P(0),Z(0), R(0),N(0)] and P_t. Using MATLAB we integrated the set of re-scaled equations to find the values [B(2π),P(2π),Z(2π), R(2π),N(2π)] after one complete period . If the solution is truly periodic, then the initial conditions should match these values. We used the equilibrium point $B_{eq} = \gamma$ as the initial value for $B(0)$ as we know a periodic solution set will include this point. We estimated the values of the other variables when $B(t) = \gamma$ using the numerical MATLAB code, and used these as initial values, including a guess for the period P_t which was also estimated from the MATLAB results.

Newton's method was used to adjust the estimates of P(0),Z(0), R(0),N(0) and P_t so that the residual quantities $B(0)-B(2\pi)$, $P(0)-P(2\pi)$, $Z(0)-Z(2\pi)$, $R(0)-R(2\pi)$ and $N(0)-N(2\pi)$ are made arbitrarily small. We used a damped version of Newton's method whereby if the norm of the vector of residuals is not reduced then the length of the correction step used in the method was halved. As limit cycles become more unstable the method finds it harder to converge to a solution. Integrating the system of equations backwards in time was found to be necessary for highly unstable solutions, since this procedure converts an unstable orbit into a stable one (in negative time).

After we have calculated a limit cycle, we then perform a linear perturbation to the system (3.11) once they have been re-scaled with respect to τ . The resultant coefficient matrix is 2π -periodic in τ and so we can use Floquet theory to ascertain the stability of the limit cycle. This method is described in Forbes (1991). In brief we found the eigenvalues of a monodromy matrix, which give a measure of how close the perturbation is to the limit cycle. If $|\lambda_i| < 1$ for all i then the limit cycle is stable. If one of the $|\lambda_i| > 1$ then the limit cycle is unstable. The result of our numerical analysis is now considered. We started with the initial set of parameter values

$$\alpha = 0.4, \beta = 0.34, \gamma = 1.2, \delta = 0.4, \eta = 0.01, c_{p0} = 0.1, c_{b0} = 0.1, N_0 = 2.$$

The locations of the Hopf points were obtained form Figure 3.1.

From Fig,3.1 we can see that as N_0 increases from 1.092 the supercritical and subcritical branches of Hopf values diverge along the β axis until they reach a minimum and maximum respectively, at about $N_0 = 2$. These two branches then begin to converge again until they meet at $N_0 = 10.82$, at which point the Hopf criteria (3.28) fail. As previously mentioned the oscillatory solutions born from a Hopf bifurcation, occur for values of β inside the the curve (Fig 3.1), for each value of N_0. We can now show the behaviour of the limit cycles born at a fixed value of N_0 as we vary β beyond the supercritical point and up to the sub critical value, as determined from Fig 3.1. This is detailed below in Fig 3.2.

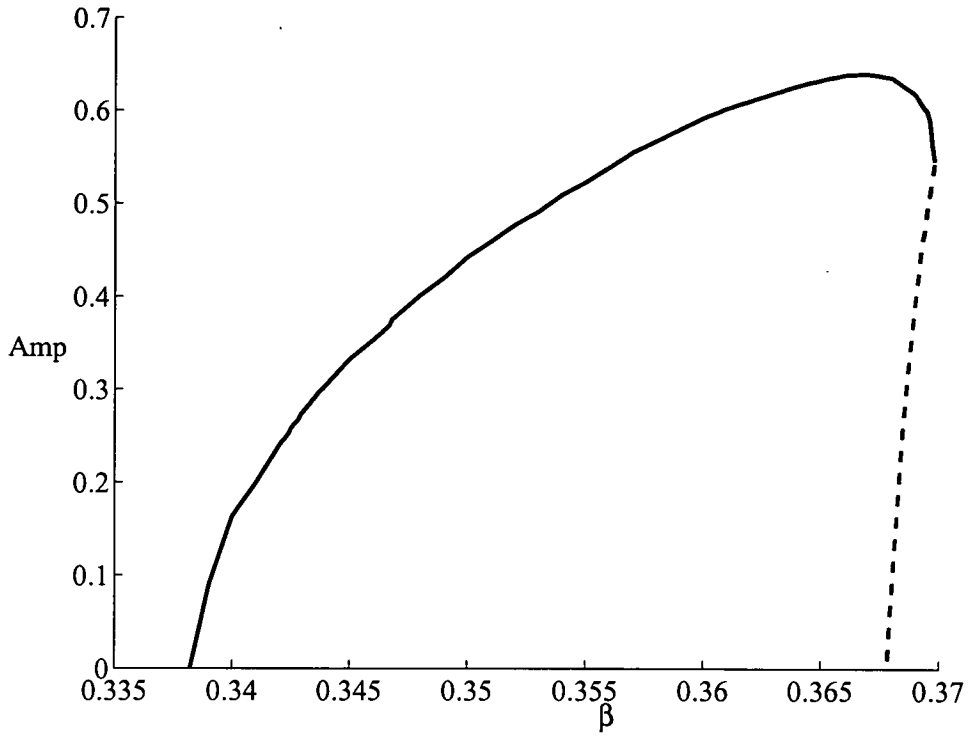

Fig 3.2: The amplitude of the limit cycles of B(t) formed at successive values of Beta for fixed $N_0 = 2$. Here $\alpha = 0.4, \gamma = 1.2, \delta = 0.4, \eta = 0.01, c_{b0} = 0.1, c_{p0} = 0.1, \mu = 0.1$

Fig 3.2 is a bifurcation diagram showing the dependence of the amplitude of the limit cycles formed for the Bacteria on the reproduction rate β. At $\beta = 0.3375$, the value predicted in Fig 3.1 for the super critical Hopf point at $N_0 = 2$, a limit cycle was found. We also checked this value by finding the eigenvalues of the Jacobian of the linear perturbation model described in (3.19), where at this value of β there exists a purely complex conjugate pair of eigenvalues. The solid line in Fig 3.2 represents the stable portion of the non-linear oscillatory solution branch. To follow this branch accurately we reduced the error tolerance (MATLAB) used for the integration solver to 10^{-9}. This was done to so as to improve numerical accuracy.

The dashed lines in Fig 3.2 are the unstable portion of the non-linear oscillatory solution branch. These limit cycles were found by integrating backward in time. As was mentioned previously, this was necessary as the limit cycles in this region were highly unstable and so the perturbation analysis failed with forward integration.

As can be seen from Fig 3.2 there is another Hopf bifurcation (sub-critical) at $\beta = 0.3675$, where once again our linear perturbation model (3.19) predicts a change should occur. Furthermore this value is in agreement with the value determined from Fig 3.1 at $N_0 = 2$ for the sub-critical Hopf point. Another feature that can be seen from Fig 3.2 is the fold bifurcation occurring at $\beta = 0.369$. This is the where the limit cycles go from stable to unstable. The Floquet matrix for the non-linear problem indicates a change here, as one of the eigenvalues for the monodromy matrix exceeds unity. What

Fig 3.2 does not display, but was determined during the construction of this diagram, is the period of each limit cycle as β varies. We found that for the super-critical hopf point, $\beta = 0.3375$, the non-dimensional period is approximately 7.2236. This equates to about 14.5 days in dimensional terms. Similarly the period for the sub-critical Hopf point, $\beta = 0.3675$, the non-dimensional period was determined to be 6.7416 or 13.5 days in dimensional terms. At the fold bifurcation the period in non-dimensional terms is 7.1079 or 14.2 days in dimensional terms.

We now look at two distinct solutions to the system occurring at the same value of β. This serves to highlight the dynamics of a complex system such as is being studied.

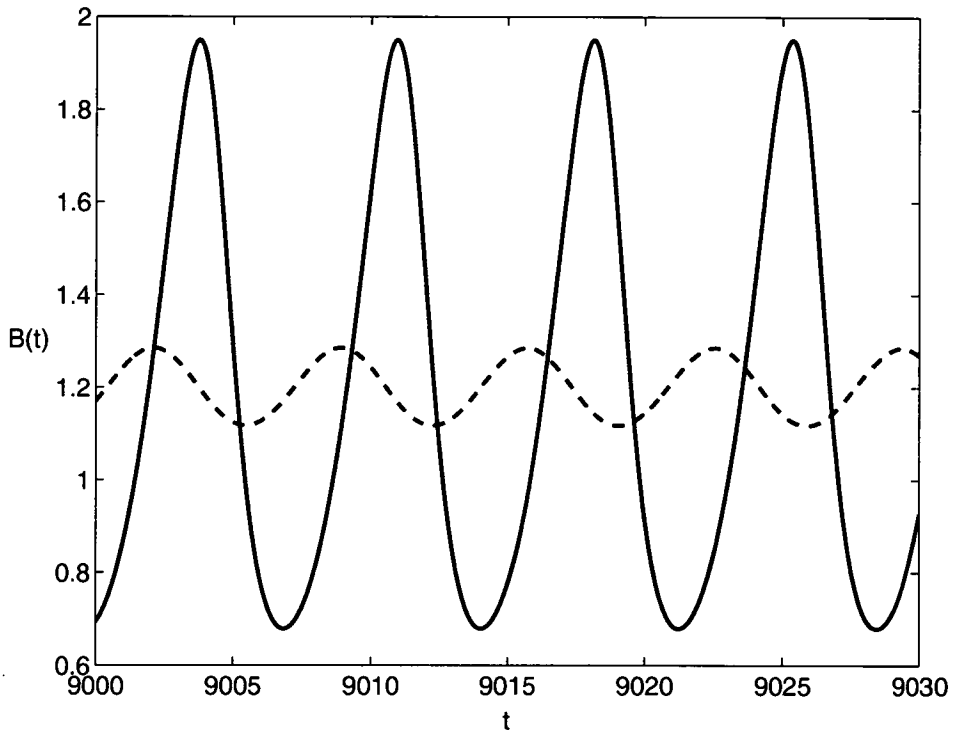

Fig 3.3: The unstable (dashed line) and stable (solid line) limit cycles for the solution B(t) at the same value of Beta=0.368.

Figure 3.3 shows that at the value $\beta = 0.368$ there are two independent solutions to the system forming two distinct limit cycles, at the same values of the physical paramters. For Bacteria at this value the stable solution is shown with a solid line. As can be seen from the graph the amplitude of the stable orbit is much greater than the unstable counterpart, consistently with Fig 3.2. That two distinct limit cycles can be formed for the same parameter value shows the complexity of the system. The assertion by Gross (2003) that the stability of a steady state can be affected by enrichment dependent on the interaction function used is not only borne out by this result, but also shows that the statement requires careful investigation due to the effects of nonlinearity in the system. We examined the stability of the two limit cycle solutions produced at $\beta = 0.368$ using Floquet theory. The results of this analysis are illustrated in the following figures.

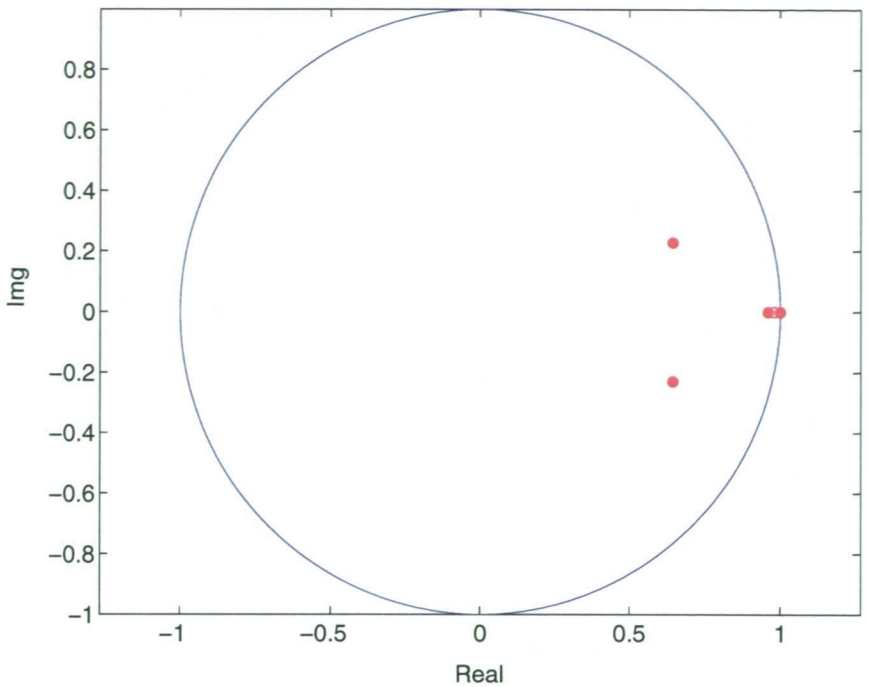

Fig 3.4 The eigenvalues of the stable limit cycle displayed on the unit circle

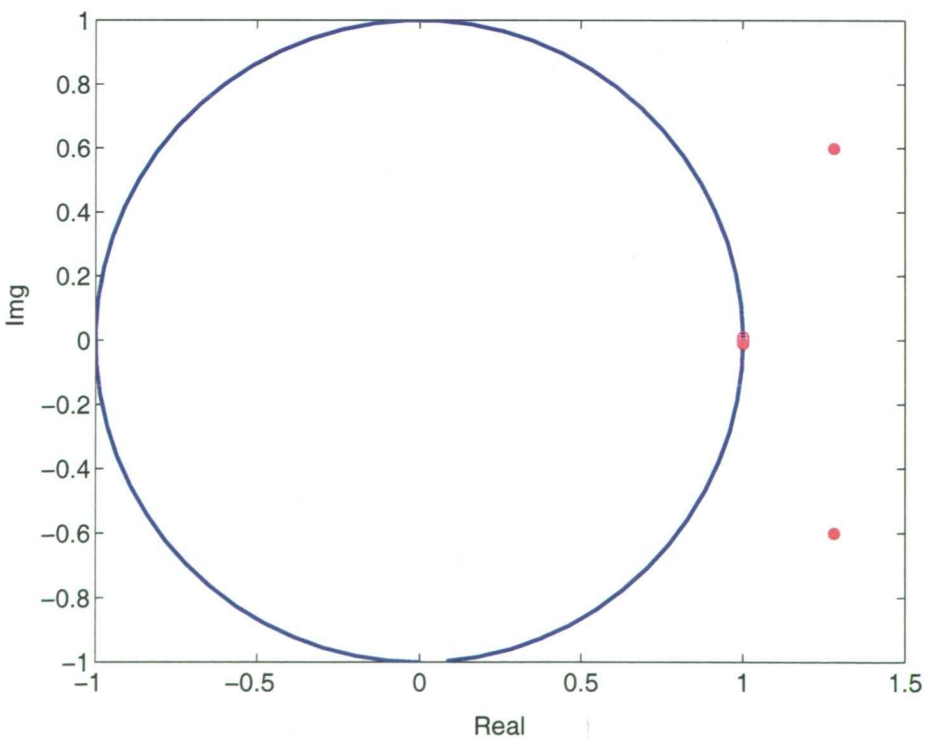

Fig 3.5 The eigenvalues of the unstable limit cycle displayed on the unit circle

Figure 3.4 shows the five eigenvalues (red dots) of the monodromy matrix formed when we solve the linear perturbation to the limit cycle. These are shown against the unit

circle $|\lambda|=1$ in the complex plane, since this represents the border between stability and instability in Floquet theory. When one of the eigenvalues crosses the unit circle the solution becomes unstable. Now in Fig 3.4 we see that one of the eigenvalues is equal to 1. It is known that, for limit cycles, one Floquet multiplier must be equal to one. Physically, this corresponds to the fact that a perturbation tangent to the limit cycle remains on it, representing a neutrally stable event (Seydel 1994). This requirement, in fact, represents a very sensitive test of the numerical accuracy of our method. All the other eigenvalues lie inside the unit circle and therefore the solution is stable. If we then consider Figure 3.5 we see that the eigenvalues (indicated by red dots) have one pair of complex conjugates with real components that are significantly greater than one. This therefore corresponds to an unstable limit cycle.
The instability of this solution means that as a result of a small perturbation ε the resultant solution will diverge from the limit cycle. In Figures 3.6 and 3.7 we can see this pronounced change in stability.

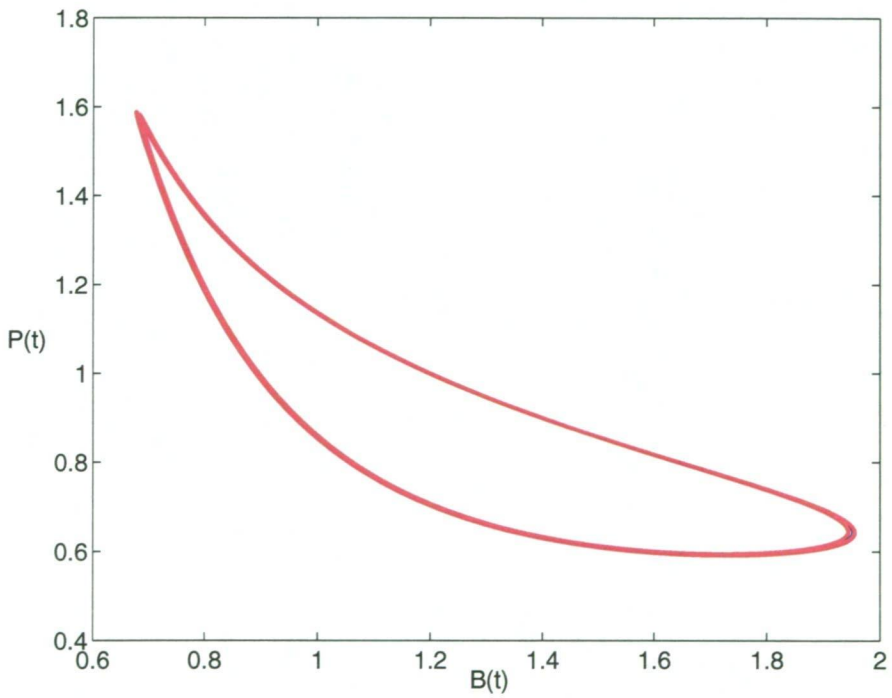

Fig 3.6. The stable limit cycle (blue) and the perturbation solutions (red) for perturbations above and below the limit cycle.

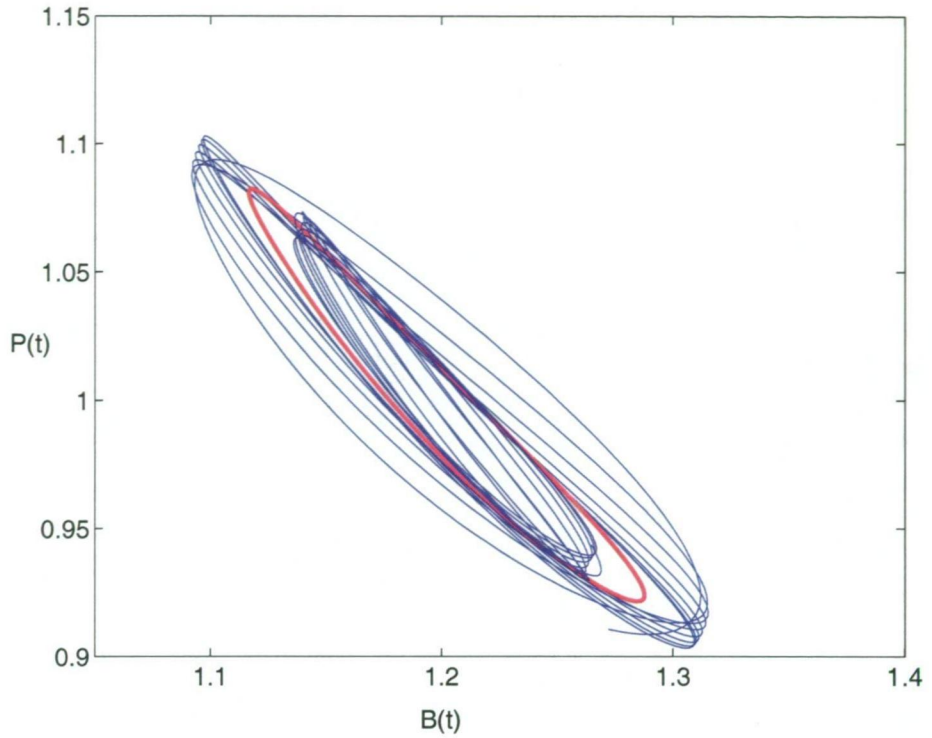

Fig 3.7 The unstable limit cycle (blue) and the perturbation solutions (red) for perturbations above and below the limit cycle.

Figures 3.6 and 3.7 show a perturbation to both the stable and unstable limit cycles formed at $\beta = 0.368$. We achieved this perturbation by changing the initial conditions by, in the first instance, adding 0.02 to the initial values of each of the four species and the nutrients and finding the solutions and in the second instance, subtracting 0.02. This is equivalent to making a perturbation outside then inside the limit cycle. Each figure shows the limit cycle run for a suitable time as well as the solutions of the perturbations to the limit cycles. From the stable case seen in Fig 3.6 we can see that the perturbation solutions converge to the limit cycle (shown in red). This is as we would expect in a stable case. In Fig 3.7 the solutions do not converge but instead oscillate and move away from the limit cycle.

3.4. Discussion

This chapter presented an investigation of the solutions to the system proposed by Stone (1990) in the case where the nutrients were allowed to vary. The system predicts four steady-states (and two more with unphysically realizable negative values for the populations). Of these equilibria, only one predicts long term survival for all four species. It is around this equilibrium point that we centred our study.

In the previous chapter the system, where nutrients are not allowed to vary, was degenerate, meaning the unforced equations gave rise to equilibrium points that are centres (excluding the point where all populations vanish). It was suggested that when nutrients are allowed to vary, that these points may become Hopf points. In the fully populated equilibrium point, Hopf bifurcations were found for a range of parameter values. Furthermore, the limit cycles found changed stability as we moved along the solution branch. The Floquet multipliers calculated for these solutions along this branch, indicated that there was no period doubling bifurcation present, typically a route to chaos, for the parameter values used.

It should also be noted that Fig 3.1 shows the Hopf curve appearing for a small value for N and disappearing as N increases beyond a certain value. The limit cycles only appear for certain parameter values and particularly when N is relatively small. We can also see from Chapter 2, there are no limit cycles when N is in abundant supply. If in fact the interaction between P and B is thought of as a de-facto defence mechanism, then although we are not modelling how this interaction works as N is varied, we still can say that the model with this interaction in place provides stable solutions for low nutrient levels.

In section 3.3 we used the values for the interaction constants stated in Stones' (1990) paper; the constants simulate the system in a stressed state so that phytoplankton releases extracellular organic carbon (EOC). Although our interpretation of the relationship between phytoplankton and bacteria is different to that of Stones' (1990), we have shown that in our case the system finds a set of stable solutions of increasing amplitude for all populations, which remains stable as the reproductive rate of bacteria increases up until the point a fold bifurcation is reached and stability is lost. We must consider the fact that we have changed the values for the interaction function η, between the bacteria and phytoplankton, making it considerably less than that derived from Stones' (1990) dimensional rate constants. Also, the range of values chosen for the reproductive rate of the bacteria β is less than that chosen by Stone (1990). These interaction functions are for the non-dimensional system (3.11). A change to β is achieved by increasing r_b and a change in η can be achieved by either increasing r_r and r_z at the same rate or by decreasing r_i. Although we have changed these values slightly to find a Hopf bifurcation we would consider it reasonable to assume that they still fall within acceptable ranges for the biological processes they represent. Stone (1990) showed that for the interaction rates used in his paper there were secondary benefits to the phytoplankton within the system as a whole. He did not analyse the system to show

its dynamics at these values. However, as mentioned our model differs slightly to Stone's (1990). This does not change the previous comment that the work of Stone (1990) does not explain the dynamics of the system and so the "secondary effects" found do not imply that the system, which supports all the species present, is actually benefited at all by the benefit to the phytoplankton. Perhaps, however, it might be beneficial to model strict commensalism between bacteria and phytoplankton to examine the dynamics of the system with this relationship.

We have chosen a Michaelis-Menten term for the nutrient uptake. There are of course other possibilities, although any law that limits the rate for large nutrient concentration might reasonably be expected to behave at least qualitatively similarly to the result s presented here. We have not considered migration or alternative models for the interaction between the bacteria and phytoplankton. Nevertheless, this study has shed some light on the dynamics of this system. In addition, we have assumed that the mass of nutrient per species is roughly constant, as indicated in equation (3.9). The dynamics of this system would no doubt become considerably more elaborate if this assumption were to be relaxed. However these are considerations for further study.

One final note should be made on the period of the limit cycles found. These periods of roughly half a month may suggest that, in order to see the complicated resonance structure in Chapter 2, diurnal forcing would no longer be appropriate. This however remains a topic for further investigation.

CHAPTER 4

Conclusion

The paper by Lewi Stone (1990) sought to offer an explanation for the paradoxical behaviour of phytoplankton. The key question was concerned with why an organism would apparently contribute to the survival of a competitor. A priori there could be many explanations. The competitor offers protection from a predator despite the competition aspect of their relationship. Stone's (1990) explanation that the Protozoa contribution to the nutrient pool is of benefit to the entire system falls under the general notion of secondary effects. However Stone's (1990) paper does not predict that the dynamics of the system show any sustainable benefit from the secondary effects he discusses. The purpose of this thesis and the dynamical systems approach that it uses is not to explain the biology of a system, but to examine a hypothesis and provide information about the system that is not initially obvious, and to provide qualitative information about the effects that changing parameters have on the system.

We began our approach by using a simple model to simulate the system described in Stone's (1990) paper. Chapter 2 dealt with the situation where nutrient concentration was considered to be constant. This situation could be found in nature in the case that nutrients are in an abundant supply. The phytoplankton stimulate the bacteria when nutrients are low; however if the nutrient concentrations are considered constant we can take this out of the equation and examine the mechanics of the top two levels of the trophic interaction. This can provide insight into the dynamics of the system at this level. We can then see how these dynamics change with the introduction of more species or more realistic interaction terms.

We found that in the case of no forcing, in chapter 2, a Hopf bifurcation leading to limit cycle behaviour is not possible. Numerical solutions found for the non-forced case did however appear as non-linear centres for the chosen parameter values. When forcing was allowed in the system then resonance peaks appeared in the solutions as well as quasi-periodicity and chaos. These conclusions have been supported by experimentation on similar systems (Shertzer et al 2002). An important point here is that we have shown the rich complexity available in a simple model and although the model is simple it does simulate many of the realistic influences found in nature such as diurnal forcing and competition. The limitations with our model are the same ones found in all biological models. These involve the questions of whether the biology has been modelled accurately, whether the system (3.10) is an appropriate representation of Stone's (1990) scheme, and whether the interactions between components in the trophic web have been modelled appropriately. These questions must ultimately be answered by biologists. Nevertheless, this thesis has shown what dynamics and behaviour can be expected, if the modelling is accurate.

In the third chapter we further developed the model by incorporating nutrient concentrations into the reproductive rates for bacteria and phytoplankton, as well as

introducing a fifth equation for the rate of change of nutrients. These changes had the effect of making the system non-degenerate. We witnessed the emergence of a supercritical Hopf-bifurcation. The limit cycles that emerged from the super critical Hopf-bifurcation were stable and increased in amplitude as β varied up until a point that the stability was lost and eventually the limit cycles vanished into a sub critical Hopf point.. This type of situation might indicate the conditions necessary for long term survival of a species. In Chapter 2 we found that there were no limit cycles resulting from a Hopf bifurcation, in the unforced system, when nutrients are in abundance. However this same unforced system does permit limit cycles when nutrients are taken into consideration, particularly at relatively low nutrient concentrations, in which case the system is capable of stability when stressed by low nutrient levels. These low Nutrient levels should be particularly damaging to the Phytoplankton with respect to the way we have modelled the interaction between it and the Bacteria. It was mentioned previously in the thesis that this interaction could be viewed as a defacto defence mechanism of the system as a whole. In the future it would important to model this interaction rate as a defence mechanism utilised by Phytoplankton and dependent on Nutrients, to see the effect on the system. We did vary two of the non-dimensional parameters from those that would have been determined from the dimensional rates found in Stone's (1990) paper. The non-dimensional amplitude of the forcing in the reproductive rate β_1 was used as the critical parameter in chapter 2 in the forced case. We saw in both chapters that as β or β_1 reached critical values the dynamics of the model changed significantly. This shows the effects that even a small change to a parameter can have on a system as a whole. This indicates the value and insight that can be derived by treating biological models from a dynamical systems point of view.

We have made several assumptions about the models developed in chapters 2 and 3. When choosing scales in the non-dimensionalisation phase, we assumed the populations can be scaled by the same factor. Secondly we assumed in chapter 3 that the species all contain roughly the same mass of nutrients per volume when forming the fifth equation. We embraced the idea that the relationship between Phytoplankton and Bacteria is symmetrical, accepting that one benefits as the other loses. To what extent these assumptions are accurate is a question that must ultimately be resolved by biologists. The dynamical systems approach deals with qualitative aspects of model behaviour, and in the past has contributed greatly to the biological sciences using even such inaccurate models as the Lotka-Volterra system. Developing mathematical models of realistic biological systems is clearly an iterative process between mathematical and biological sciences.

Further work on the model could take place in the area of modelling a commensal relationship between bacteria and phytoplankton to see the effect on the dynamics. Other considerations could be the introduction of more realistic interaction functions (delay terms) or introducing terms for migration. What cannot be misinterpreted is the effect of the non-linearity in the system and the way that the tools available in dynamical systems theory have been used to predict phenomena that are observable in the physical world.

References

Edelstein-Keshet (1988) Mathematical Models in Biology, Random House, NY

Edwards AM, Brindley J (1999) Zooplankton mortality and the dynamical behaviour of plankton population models. Bull Math Biol 61:303-339.

Edwards AM (2001) Adding detritus to a nutrient-phytoplankton-zooplankton model: A dynamical systems approach. Jour Plan Res 23: 389-413.

Forbes LK (1991) Forced transverse oscillations in a simple spring-mass system, Siam Jour App Math. 51:1380-1396.

Freund JA, Mieruch S, Scholze B (2006) Bloom dynamics in a seasonally forced phytoplankton-zooplankton model. Ecol Comp 3:129-139.

Gross T, Ebenhoh W, Feudel U (2004) Enrichment and foodchain stability: The impact of different forms of predator-prey interaction. J Theor Biol 227:349-358

Guckenheimer J, Holmes P (1983) Nonlinear Oscillations, Dynamical Systems and Bifurcations of Vector Fields, Springer-Verlag, NY

Huppert A, Olinky R, Stone L (2004) Bottom-Up excitable models of phytoplankton blooms. Bull Math Biol 66:865-878

Hutchison GE (1961) Paradox of the plankton, Amer Nat 95:137-145
Jansen VAA (2001) The dynamics of two diffusively coupled predator-prey populations.
Theo Pop Biol 59:119-131

Kirk KL (1998) Enrichment can stabilize population dynamics: Autotoxins and density dependence Ecology (USA) 79:2456-2462

Medio L, Lines M (2001) Nonlinear dynamics a primer. University Press, Cambridge

Murray JD (1989) Mathematical Biology. Springer-Verlag, NY

Ruan SG (2001) Oscillations in plankton models with nutrient recycling
Jour Theo Biol 208:15-26

Scheffer M, Rinaldi S, Huisman J, Weissing FJ (2003) Why plankton communities have no equilibrium; solutions to the paradox, Hydrobiologia 491: 9-18

Seydel R (1994) Practical Bifurcation and Stability Analysis: From equilibrium to chaos 2nd Edition. Springer-Verlag, NY.

Shertzer KW, Ellner SP, Fussman GF, Hairston NG (2002) Predator–prey cycles in an aquatic microcosm, Jour Anim Ecol 71:802-815.
Sprott JC, Wildenberg JC, Azizi Y (2005) A simple spatiotemporal chaotic Lotka-Volterra model. Chaos Solitons and Fractals 26: 1035-1043

Stone L (1990) Phytoplankton-bacteria-protozoa interactions: a qualitative model portraying indirect effects. Mar Ecol Prog Ser 64:137-145

Thompson JMT, Stewart HB (1989) Nonlinear Dynamics and Chaos, John Wiley and Sons NY

Truscott JE, Brindley J (1994) Ocean plankton populations as excitable media, Bull Math Biol 56:981-998

Van der Stap I, Vos M, Tollrian R, Mooij WM (2008) Inducible defences, competition and shared predation in planktonic food chains, OECO 157:697-705

Verschoor AM, Vos M, van der Stap I (2004) Inducible defences prevent strong population fluctuations in bi- and tritrophic food chains, Ecol Lett 7:1143-1148

Wang HL, Feng JF, Shen F, Sun J (2005) Stability and bifurcation behaviours analysis in a non-linear harmful algal dynamical system, App Math Mech 26:729-734
Sprott JC, Wildenberg JC, Azizi Y (2005) A simple spatiotemporal chaotic Lotka-Volterra model. Chaos Solitons and Fractals 26: 1035-1043